ENCLOSURE 3

NON-PROPRIETARY VERSION

HOLTEC REPORT HI-971708

CRITICALITY SAFETY EVALUATION OF THE SPENT FUEL STORAGE RACKS IN THE DUANE ARNOLD ENERGY CENTER FOR MAXIMUM ENRICHMENT CAPABILITY

HOLTEC INTERNATIONAL

AUGUST 1997

65 Pages Follow

CRITICALITY SAFETY EVALUATION OF THE

SPENT FUEL STORAGE RACKS in the DUANE ARNOLD ENERGY CENTER

FOR MAXIMUM ENRICHMENT CAPABILITY

Prepared for the

DUANE ARNOLD ENERGY CENTER

by

Stanley E. Turner, PhD, PE

August 1997

Holtec Project 60884
Holtec Report HI-971708

HOLTEC INTERNATIONAL

230 Normandy Circle
Palm Harbor, FL 34683

555 Lincoln Dr. W.
Marlton, NJ 08053

HOLTEC INTERNATIONAL

Holtec Center, 555 Lincoln Drive West, Marlton, NJ 08053
Telephone (609) 797-0900
Fax (609) 797-0909

REVIEW AND CERTIFICATION LOG

DOCUMENT NAME:	Criticality Safety Evaluation of the Spent Fuel Storage Racks in the Duane Arnold Energy Center for Maximum Enrichment Capability
HOLTEC DOCUMENT I.D. NUMBER:	HI-971708
HOLTEC PROJECT NUMBER:	60884
CUSTOMER/CLIENT:	IES Utilities

REVISION BLOCK

REVISION NUMBER*	AUTHOR & DATE	REVIEWER & DATE	QA & DATE	APPROVED† & DATE	DIST.‡
ORIGINAL	S.B. TURNER 8/15/97	John C. Wagner 8/22/97	M. PURDO	S.B. TURNER 8/22/97	C
REVISION 1					
REVISION 2					
REVISION 3					
REVISION 4					
REVISION 5					

This document conforms to the requirements of the design specification and the applicable sections of the governing codes.

Note: Signatures and printed names are required in the review block.

* A revision of this document will be ordered by the Project Manager and carried out if any of its contents is materially affected during evolution of this project. The determination as to the need for revision will be made by the Project Manager with input from others, as deemed necessary by him.

† Must be Project Manager or his designee.

‡ Distribution: C: Client
M: Designated Manufacturer
F: Florida Office

THE REVISION CONTROL OF THIS DOCUMENT IS BY A "SUMMARY OF REVISIONS LOG" PLACED BEFORE THE TEXT OF THE REPORT.

Form: RCL.02

TABLE OF CONTENTS

List of Tables

List of Figures

1.0 INTRODUCTION and SUMMARY

The spent fuel storage racks in the Duane Arnold Energy Center include racks designed by the PaR Corporation and by Holtec International. These racks were originally designed to accommodate fuel of lower enrichment than might be expected to be used in the future. The present study was undertaken to determine the maximum enrichment capability for safe storage of spent fuel in the racks. To ensure completeness, the study encompasses all of the fuel types currently in use and those planned for possible future use at Duane Arnold. Some of the advanced fuel designs, specifically fuel of the higher enrichments, have not been fully developed and required gadolinia loadings have not yet been established. However, it has long been known, and calculations herein confirm, that the use of the infinite multiplication factor (k_{inf}) in the standard core geometry* (also called core k_{inf}) allows fuel acceptance criteria to be defined in terms of the peak core k_{inf} over burnup.

The PaR racks at Duane Arnold had been very conservatively designed and calculations reported here confirm that the racks are capable of safely accepting all fuel assemblies previously used or that may be used in the future, with enrichments up to 4.95 wt% U-235**, assuming a conventional loading of gadolinia. Although the design of the Holtec racks[1] is less conservative, criteria are also presented in this report for fuel with enrichments up to 4.95%. Results of the analyses for the most reactive fuel assembly type (GE-12, 10x10 array) are summarized in Figure 1.1 for both rack types, in terms of the k_{inf} in the standard core geometry. The data for the GE-12 fuel conservatively bounds all other fuel types and enrichments.

---

* The k_{inf} in the standard core geometry is usually provided by the fuel vendor and is defined as the infinite multiplication factor in the uncontrolled core geometry (normal lattice spacing) at 20° C without voids.

** Because of power peaking, it is not likely that fuel with average enrichments exceeding 4.6% will become available in the foreseeable future.

Three different fuel types were evaluated: (1) the GE-10, 8x8 rod bundle, (2) the GE-13, 9x9 rod bundle, and (3) the GE-12, 10x10 rod bundle. The GE-10 is currently the most prevalent fuel type at Duane Arnold. Figure 1.2 illustrates the effect of initial enrichments on the maximum reactivity in the PaR storage racks, conservatively including the effect of calculational and mechanical uncertainties (tolerances). Figure 1.3 presents the corresponding data for the Holtec racks.

The criteria for acceptable storage of fuel in the Duane Arnold storage racks are as follows:

Either a maximum lattice-average enrichment less than the following–

	PaR Racks	Holtec Racks
GE-10, 8x8 array	<4.45% Enrichment	<3.34% Enrichment
GE-13, 9x9 array	<4.40% Enrichment	<3.34% Enrichment
GE-12, 10x10 array	<4.35% Enrichment	<3.28% Enrichment

or a maximum (peak) cold (20°C) uncontrolled k-infinity less than 1.39 for the PaR racks or less than 1.29 for the Holtec racks in the standard core geometry (evaluated for 40% void fraction during core depletion), as reported by the fuel vendor.

In the PaR racks, any fuel assembly with an enrichment less than or equal to 4.95% that has accumulated a burnup of at least 4 MWD/KgU burnup (2 MWD/KgU for 4.60% fuel) or more is also acceptable for storage, regardless of the enrichment or number and loading of gadolinia rods.

Results reported here include the effect of part-length fuel rods used in the GE-13 (9x9 array) and GE-12 (10x10 array) designs and are presented in terms of the lattice average enrichment. Vendor (GE) calculations usually report the lattice average enrichment and the cold, uncontrolled k_{inf} in the standard core geometry. In this report, when reactivities are referenced to the k-infinity in the standard core geometry, an additional allowance of $0.01\Delta k$ is added to compensate for any differences that may exist between the vendor (GE) calculations and those reported here.

Calculational uncertainties and manufacturing tolerances are also included, as required by SRP 9.1.2 and Regulatory Guide 1.13 (Rev.2). Abnormal and accident conditions were also considered to assure safe operation under all credible conditions.

Examination of available data for fuel bundles currently at the Duane Arnold Energy Center confirms that all fuel assemblies are well within the acceptance criteria for storage in either the PaR or the Holtec racks.

Gadolinia burnable poison within certain fuel rods in an assembly reduces reactivity during the early stages of burnup until the gadolinium is almost completely depleted. The peak in reactivity occurs at a fuel burnup that depends upon the number and loading of the gadolinia bearing rods. For a given fuel enrichment, an increase in either the number of gadolinia rods or their loading will increase the burnup at which the peak reactivity occurs and reduce the value of the peak reactivity. Thus, an increase in the number of gadolinia rods or their loading will always be more conservative and therefore acceptable.

2.0 ANALYTICAL CRITERIA and ASSUMPTIONS

2.1 Fuel Assembly Specifications

Three different fuel assembly configurations were assumed in the analyses, as follows:

- GE-10 8x8 fuel assemblies with a single large water rod replacing 4 fuel pins,
- GE-13, 9x9 fuel assemblies with 2 water holes replacing 7 fuel rods, and
- GE-12, 10x10 fuel assemblies with 2 large water rods replacing 8 fuel rods.

The GE-12 and GE-13 fuel assemblies contain part-length rods, creating an array of higher water-to-fuel ratio near the top. Specifications for the fuel assemblies are summarized in Table 2.1. Of the various fuel assembly types investigated, the GE-12, 10x10 rod assembly was found to be the most reactive. All of the GE fuel assemblies have natural UO_2 blankets at each end. The calculations reported here do not include blankets, and are based on the lattice-average (planar) enrichments. The blankets, therefore, do not contribute to the calculated reactivities. Blankets of natural UO_2 would result in lower and more conservative reactivities (k_{eff}) for the entire assembly. Fuel enrichments, as used in this report, refer to the enriched lattices in the assembly without consideration of any axial blankets that might be present.

Calculations were also made to determine the effect of removing the zircalloy flow channel. Results showed a decrease in reactivity with removal of the flow channel (-0.0027 Δk for the PaR racks and -0.0098 Δk for the Holtec racks). Therefore, the reactivity with the flow channel installed on the assembly yields the higher and controlling reactivity.

2.2 Storage Rack Specifications

The nominal spent fuel storage cell used for the criticality analyses of the PaR racks is shown in Figure 2.1. The rack is composed of 0.125 inch thick aluminum boxes of 6.156" I.D. A Boral absorber panel is located between boxes in a 0.2185 inch cavity. The fuel assemblies are assumed to be centrally located in each storage cell on a lattice spacing of 6.625 ± 0.050 inches. The Boral absorbers have a core thickness of 0.080 inches with a minimum loading of 0.0232 g B-10/cm^2 (nominally 0.025 g B-10/cm^2 and are clad on both sides with 0.0175-inch thick aluminum.

Figure 2.2 illustrates a typical cell in the Holtec racks, with a Boral absorber of 0.0162 g B-10/cm^2 nominal loading. The racks consist of 0.060 inch thick stainless steel boxes on a 6.06 inch lattice spacing with a 5.90 inch inside opening.

2.3 Assumptions

In addition to the assumption that the design basis information described above is correct, the following conservative assumptions were made:

- The racks are assumed to contain the most reactive fuel for the case being analyzed, without any control rods or burnable poison, except gadolinia, as appropriate.
- The fuel assemblies were conservatively evaluated for uniform average enrichment, i.e., the distribution in enrichments normally used in BWR fuel was represented by an average.
- The moderator is assumed to be pure, unborated water at a temperature corresponding to the highest reactivity (4° C)
- Criticality safety analyses are based upon the assumption of an infinite array of storage cells in the radial direction, i.e., no credit is taken for radial neutron leakage

- Neutron absorption in minor structural members is neglected, i.e., spacer grids are assumed to be replaced by water.

- In the CASMO3 model, the flow channel was homogenized with the immediately surrounding water.

3.0 MANUFACTURING TOLERANCES and UNCERTAINTIES

3.1 PaR Racks

The affects of various manufacturing tolerances on reactivity for the PaR racks are summarized in Table 2.2 and include the following:

- Tolerance in B-10 loading in the Boral: The boron content of the Boral panels is nominally 0.025 with an uncertainty of ± 0.0018 g/cm^2. CASMO3 calculations for the minimum B-10 loading (0.0232 g/cm^2) increased the reactivity by 0.0053 Δk (manufacturing uncertainty). This estimate was confirmed by independent KENO5a calculations.

- Tolerance in Lattice Spacing: The tolerance in lattice spacing is ± 0.05 inch, assumed to result from the corresponding tolerance on the box inner dimension. Differential CASMO3 calculations, with the maximum tolerance, resulted in a reactivity increment (uncertainty) of 0.0027 Δk.

- Tolerance in Fuel Enrichment: The tolerance in fuel enrichment is assumed to be ± 0.05%, resulting in a reactivity uncertainty of ± 0.0022 Δk.

- Tolerance in UO_2 Density: The UO2 density tolerance was assumed to result in a maximum of 98% T.D. or 10.741 g/cc. Differential CASMO3 calculations resulted in a tolerance reactivity uncertainty of ± 0.0022 Δk.

- Fuel Eccentricity: The fuel assemblies are normally assumed to be located in the center of the storage cell. Calculations were made assuming the assemblies were eccentrically positioned toward the corner of the cell creating a configuration of maximum eccentricity. In KENO5a calculations, the eccentric position resulted in a reduction in reactivity and the central position is, therefore, the more conservative.

- Flow Channel Removal: Calculations were made, assuming the Zircalloy flow channel was not present. Results showed that removing the flow channels causes a reduction in reactivity, and the condition with the channel installed yields the higher and controlling reactivity.

- Tolerance in Clad Thickness: The tolerance in clad thickness is unusually large and differential CASMO3 calculations resulted in a 0.0081 Δk uncertainty.

- Tolerance in Water Rod Thickness: Calculations for the reported water rod thickness tolerance resulted in a ± 0.0003 Δk uncertainty in reactivity.

3.2 Holtec Racks

The uncertainties and allowances previously evaluated for the Holtec racks were assumed to remain applicable. The combined uncertainties from reference 1 are 0.0145 Δk with an additional allowance of 0.01 Δk for possible differences with vendor calculations.

4.0 CALCULATIONAL METHODOLOGY

4.1 Computer Codes

The principal methods of analysis were the NITAWL-KENO5a[2] code package, a three dimensional Monte Carlo code package using the 238-group SCALE cross-section library, and the CASMO3[3] code, a two-dimensional multi-group transport code for assemblies. NITAWL-KENO5a has been extensively benchmarked (see Appendix A), resulting in a bias of 0.0042 ± 0.0010 (95%/95%[4]). Independent check calculations were made with the MCNP[5] code developed by the Los Alamos National Laboratory.

In the geometric model used in the calculations, each fuel rod and its cladding were described explicitly. Reflecting boundary conditions (zero neutron current) were used in the radial direction which has the effect of creating an infinite radial array of storage cells. The KENO5a calculational model represented the part-length fuel rods in a 3-dimensional calculation and was used to develop a correction to the two-dimensional CASMO3 depletion calculations, normalizing the results to the three-dimensional model with part-length rods, where appropriate.

Since Monte Carlo calculations (KENO5a) inherently include a statistical uncertainty due to the random nature of neutron tracking, a minimum of 1×10^6 neutron histories were accumulated in each calculation. Uniform average enrichments were used in the analyses, primarily because this assumption provides conservative results and actual distributions in enrichments have not yet been developed for the higher enrichment fuel. Similarly, in most cases, the Gd_2O_3 normally used in BWR fuel assemblies was not included in the calculations, again because the distribution and loadings have not yet been developed. This approach is the equivalent of neglecting any residual gadolinium at the peak reactivity over burnup.

When defining fuel acceptable for storage in terms of the k_{inf} in the cold standard core geometry, the distribution in enrichments and the Gd_2O_3 loading are of secondary importance,

since the core k_{inf} and the rack k_{inf} are both affected in the same way. These parameters are, however, very important in determining the achievable peak reactivity over burnup. The average enrichment and the void content during core operation both affect the neutron spectrum and are more significant since they directly affect the production of plutonium during core operations.

4.2 Independent Verification Calculations

The MCNP code[9] was used to independently verify several of the KENO5a calculations. The resulting bias corrected values are listed below:

Case	MCNP	KENO5a
GE-10 @ 4.6% E (fully rodded)	0.9448 ± 0.0014	0.9442 ± 0.0012
GE-13 @ 4.6% E	0.9448 ± 0.0014	0.9440 ± 0.0012
GE-12 @ 4.6% E	0.9452 ± 0.0014	0.9457 ± 0.0012
GE-10 @ 4.4% E	0.9368 ± 0.0014	0.9353 ± 0.0012
GE-13 @ 4.6% E (partly rodded)	0.9523 ± 0.0014	0.9507 ± 0.0012
GE-12 @ 4.6% E (partly rodded)	0.9568 ± 0.0014	0.9564 ± 0.0012

These calculations are in good agreement (within the normal statistical variation) and confirm the reference KENO5a calculations.

5.0 ANALYTICAL RESULTS

5.1 Normal Storage Conditions in the PaR Racks

5.1.1 Existing Fuel Assemblies in the PaR Racks

The three most reactive fuel assemblies currently at Duane Arnold were specifically evaluated in the PaR racks. These are GE-10 assemblies, with an 8x8 array of fuel rods and a single large water rod displacing four fuel rods. Figure 5.1 shows the results of these calculations, confirming that the peak reactivity over burnup is substantially below the regulatory limit. The three fuel assemblies evaluated were:

[

]

The three assemblies described above, and all other fuel assemblies now existing at Duane Arnold, have enrichments well below the maximum allowed for the PaR racks (see Figures 1.1 or 1.2). These calculations, therefore, confirm that the PaR storage racks can safely accommodate all existing fuel assemblies within the regulatory guidelines.

Equally important are the data shown in Figure 5.2, showing the results in terms of the k_{inf} in the standard core geometry for the PaR racks. These data show that, for the existing GE-10 fuel at Duane Arnold, the racks could safely accommodate the current low enrichment fuel with a k_{inf} in the standard core geometry up to at least 1.40 (see also Figures 1.1 and 1.2).

5.1.2 Fuel of Advanced Designs and Higher Enrichments

Calculations were made for fuel of higher enrichments than those previously used and for fuel of advanced designs. For these advanced fuel concepts, neither a distribution in enrichments nor a gadolinia loading has been developed. In BWR fuel, there is a need for distributed enrichments to avoid power peaking problems, and, since 5.0% is the maximum enrichment allowed for any single fuel pin, it is not likely that a BWR fuel assembly will exceed an average enrichment of about 4.6%. Representative calculations for all three designs, with an average enrichment of 4.60% were made and the results are summarized in Figures 5.3 and 5.4. Figure 5.3 illustrates the decrease in reactivity with burnup without credit for gadolinia and indicates that a burnup of 2 MWD/KgU or more would be adequate to allow safe storage of any of the three fuel types. Any reasonable gadolinia loading would reduce the reactivity sufficient to allow safe storage. Figure 5.4 shows the relationship between the reactivity in the rack and the standard core k-infinite. This data shows that any fuel with an enrichment of 4.6% or less and a k-infinite in the standard core geometry less than or equal to 1.40* would allow the assembly to be acceptable for unrestricted storage.

Similar calculations were also made for fuel of 4.95% enrichment in the PaR racks and the results are summarized in Figures 5.5, 5.6 and 5.7. Figure 5.5 shows the decrease in reactivity with burnup and indicates that a fuel burnup of only 2 to 3 MWD/KgU would enable fuel of 4.95% average enrichment to be safely stored. Even a minimum gadolinia loading would be adequate to reduce the reactivity of fuel with 4.95% enrichment to an acceptable level. To illustrate this, calculations were made (Figure 5.6) with 7 gadolinia rods, each with 4.0% gadolinia**. For fuel of 4.95% enrichment, the actual gadolinia would be expected to be considerably greater which would reduce the peak reactivity in the rack.

---

* A k-infinite limit of 1.39 in the PaR racks is recommended in order to accommodate fuel up to 4.95% enrichment (see Figure 5.7).

** This loading of gadolinia is that used for fuel of 3.57% average enrichment (see Figure 5.1).

Figure 5.7 shows the variation in rack reactivity for the three fuel designs with fuel of 4.95% enrichment. Each fuel design is illustrated by calculations with (dotted lines) and without gadolinia (solid lines). The calculations with and without gadolinia are essentially the same when represented in terms of the k-infinite in the standard core geometry. These data confirm that calculations without gadolinia are valid when results are expressed in terms of the standard core k-infinite. For the most reactive fuel type (GE-12, 10x10 array), the limiting standard core k-infinite is 1.39 and any assembly with a standard core k-infinite of 1.39 or less would be acceptable for storage regardless of the fuel type or burnup.

5.2 Normal Storage Conditions in the Holtec Racks

Calculations were made with fuel of 4.6% and 4.95% enrichments for all three fuel types in the Holtec racks. Figure 5.8 illustrates the burnup dependent reactivities for the highest enrichment (4.95%) with an assumed gadolinia loading (7 gadolinia rods of 4.0%) for illustrative purposes. While this loading would be adequate, the actual gadolinia content, in number and loading, would be expected to be greater with a substantially lower peak reactivity in the racks. Figures 5.9 and 5.10 illustrate the variation in rack reactivity with the standard core k-infinity for 4.6% and 4.95% enriched fuel. For the limiting case of 4.95% enrichment in GE-12 fuel assemblies, the recommended peak reactivity limit in the standard core geometry is 1.29. In the original analysis (Reference 1), the recommended k-infinity limit was 1.31, based on fuel of 4.6% enrichment in an 8x8 array. The present analysis includes the GE-12, 10x10 array, with enrichments up to 4.95% and encompass the part-length fuel rods in the GE-13 and GE-12 fuel designs.

5.3 Accident/Abnormal Conditions

Reactivity consequences of accident/abnormal conditions are listed in Table 5.1 and described below:

5.3.1 Temperature and Void Reactivity Effects

The temperature and void coefficients of reactivity are negative as illustrated in Table 5.2. Consequently, the maximum reactivity occurs at a water density of 1.0 g/cc and 4°C was used as the design basis temperature. This assures that, regardless of future temperature changes, the reactivities will be bounded.

5.3.2 Eccentric Position of Fuel Assemblies

The reactivity effect of eccentric fuel positioning was evaluated for movement of the assembly toward the corner of the cell, creating an array of four assemblies at the closest possible approach. KENO5a calculations confirmed that the centered position is the most reactive in both the PaR and the Holtec racks and eccentricity in any direction reduces reactivity.

5.3.3 Dropped Fuel Assembly

A dropped fuel assembly will come to rest horizontally on top of the rack, separated by more than 12 inches from the active fuel in storage. This separation distance is more than adequate to assure no appreciable increase in reactivity. Thus, the reactivity consequences of this postulated accident are negligible. Should the dropped assembly be postulated to enter a filled cell vertically, it could impact a stored fuel bundle. Such a vertical impact would at most cause a small compression of the stored bundle, reducing the water-to-fuel ratio and thereby reducing reactivity. Consequently, a dropped fuel bundle will have a negligible impact on reactivity.

5.3.4 Seismic Event

Rack behavior under the influence of a seismic event has not been evaluated. External rack structure for the PaR racks would preclude close approach of the several modules or of the Holtec racks and a seismic event would have a negligible impact on reactivity.

5.3.5 Fuel Mis-location Event

In the unlikely event that an accidental attempt was made to place a fuel assembly outside of a storage rack module, the presence of rack structural elements on the outside of the PaR racks would prevent the offending assembly from being positioned close to the fuel. Under these circumstances, the reactivity effect would be negligible. Previous analyses[1] have confirmed that the reactivity effect of a fuel mis-loading event in the Holtec racks is also negligible.

6.0 REFERENCES

1. "Licensing Report for Spent Fuel Storage Capacity Expansion Duane Arnold Energy Center", Holtec International Report HI-92889 (undated).

2. R.M. Westfall, et. al., "NITAWL-S: Scale System Module for Performing Resonance Shielding and Working Library Production" in SCALE: A Modular Code System for Performing Standardized Computer Analyses for Licensing Evaluation, NUREG/CR-0200, 1979.

   L.M. Petrie and N.F. Landers,"KENO 5a. An Improved Monte Carlo Criticality Program with Supergrouping" in SCALE: A Modular Code System for Performing Standardized Computer Analyses for Licensing Evaluation, NUREG/CR-0200, 1979

3. M. Edenius and A. Ahlin, "CASMO-3: New Features, Benchmarking, and Advanced Applications", Nuclear Science and Engineering, 100, 342-351, (1988).

   A. Ahlin, M. Edenius, H. Haggblom, "CASMO - A Fuel Assembly Burnup Program," AE-RF-76-4158, Studsvik report (proprietary).

   A. Ahlin and M. Edenius, "CASMO - A Fast Transport Theory Depletion Code for LWR Analysis," ANS Transactions, Vol. 26, p. 604, 1977.

   "CASMO-3 A Fuel Assembly Burnup Program, Users Manual", Studsvik/NFA-87/7, Studsvik Energitechnik AB, November 1986.

4. M.G. Natrella, Experimental Statistics, National Bureau of Standards, Handbook 91, August 1963.

5. J.F. Briesmerister, Ed, "MCNP - A General Monte Carlo N-particle Transport Code, Version 4a," Los Alamos National Laboratory, LA-12625-M, 1993.

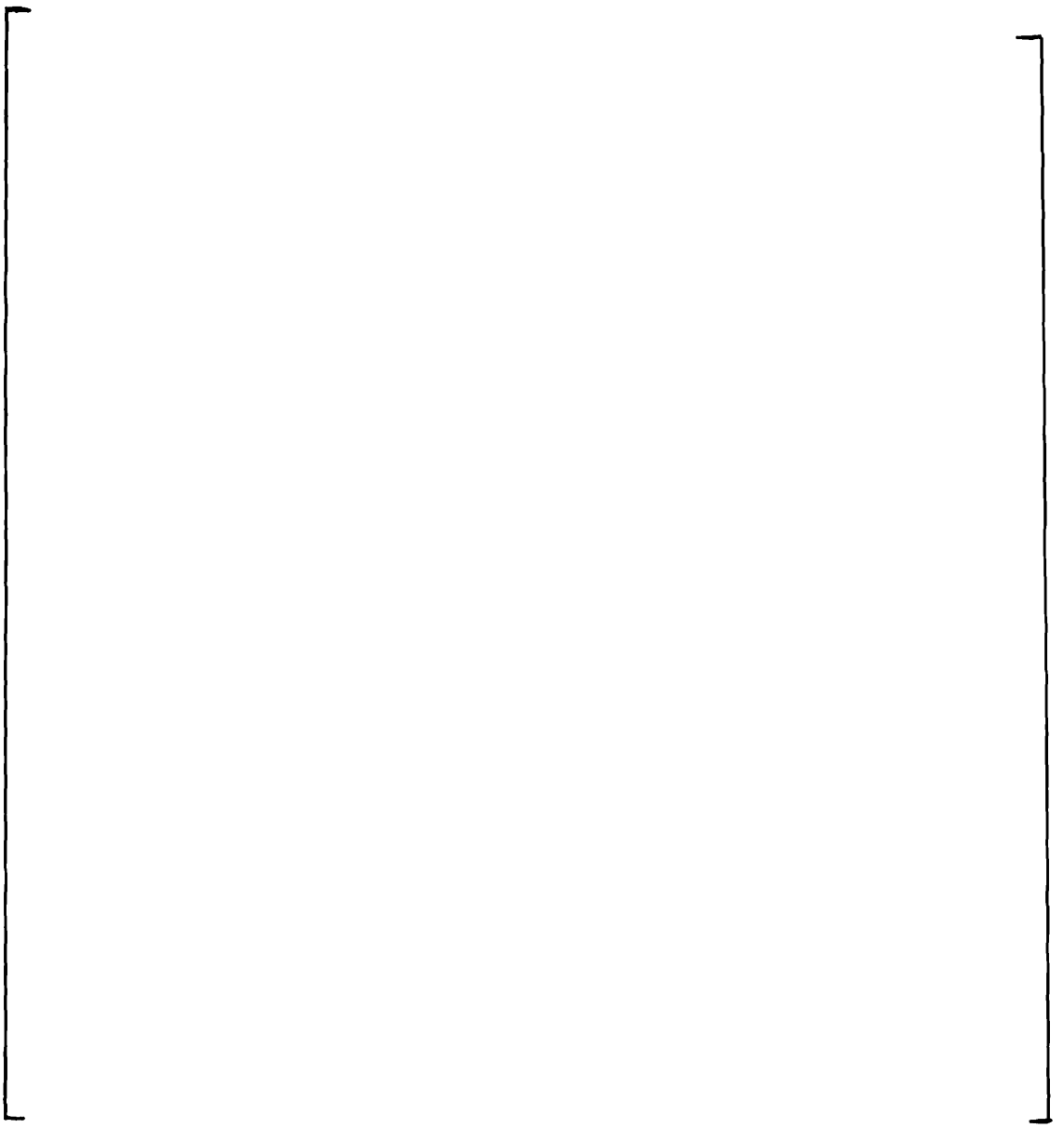

Table 2.2

SUMMARY OF MANUFACTURING UNCERTAINTIES IN THE PaR RACKS

Parameter	Delta k
Boral width	—
Boral loading	± 0.0053
Clad Thickness	± 0.0075
Lattice spacing	± 0.0027
Fuel enrichment	± 0.0022
Fuel density	± 0.0022
Water Rod Thickness	± 0.0003
Removal of flow channel	negative
Eccentric Assembly Position	negative
Statistical combination[1] of uncertainties	±0.0098
With KENO5a variation	±0.0099

[1] Square root of sum of squares of all independent tolerance effects.

Table 5.1

REACTIVITY EFFECTS OF ABNORMAL AND ACCIDENT CONDITIONS

Accident/Abnormal Condition	Reactivity Effect
Temperature increase	Negative (Table 5.2)
Void (boiling)	Negative (Table 5.2)
Assembly dropped on top of rack	Negligible
Assembly dropped into filled cell	Negative or Negligible
Movement of rack modules	No effect
Misplacement of a fuel assembly	Negligible

Table 5.2

EFFECT OF TEMPERATURE AND VOID ON CALCULATED REACTIVITY OF STORAGE RACK

Case	Incremental Reactivity Change, Δk	
	PaR Racks	Holtec Racks
4°C	Reference	Reference
20°C	-0.0021	-0.0025
70°C	-0.0117	-0.0130
120°C	-0.0248	-0.0263
120° + 10% void	-0.0495	-0.0504

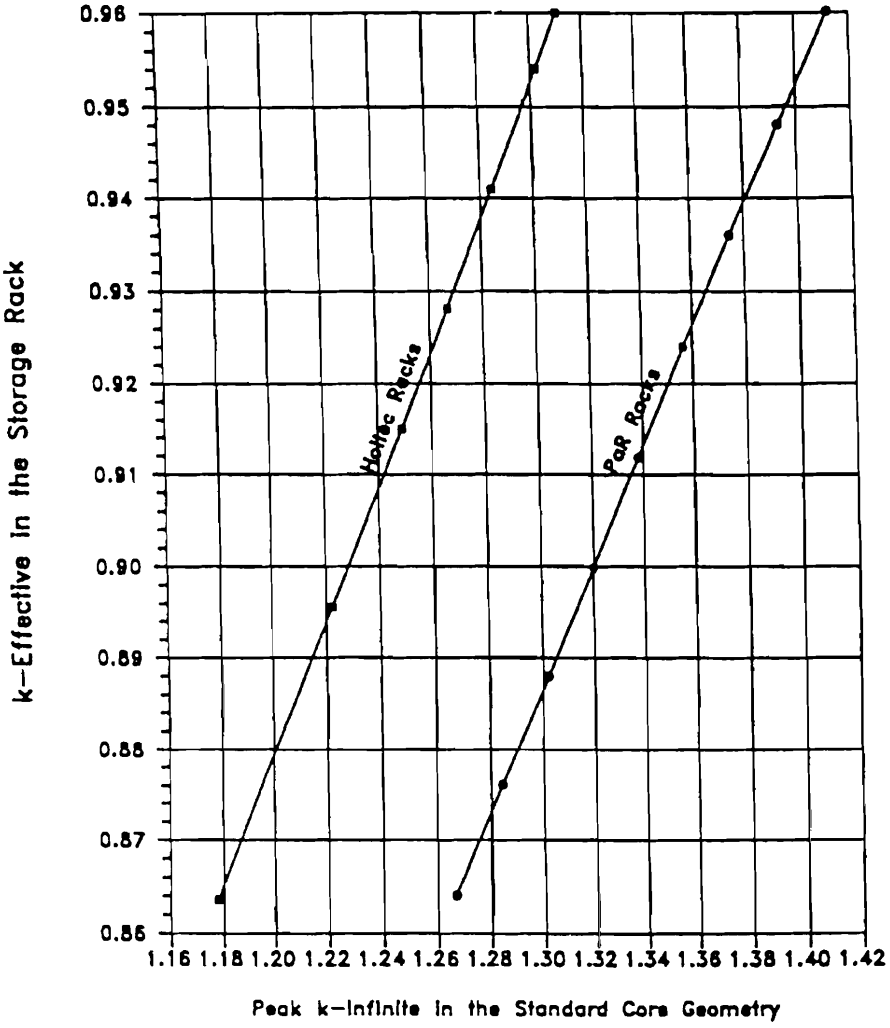

Fig. 1.1 Relationship between k-effective in the Rack and Peak k-infinite over Burnup in the Standard Core Geometry (GE-12 Fuel - Bounding Conditions)

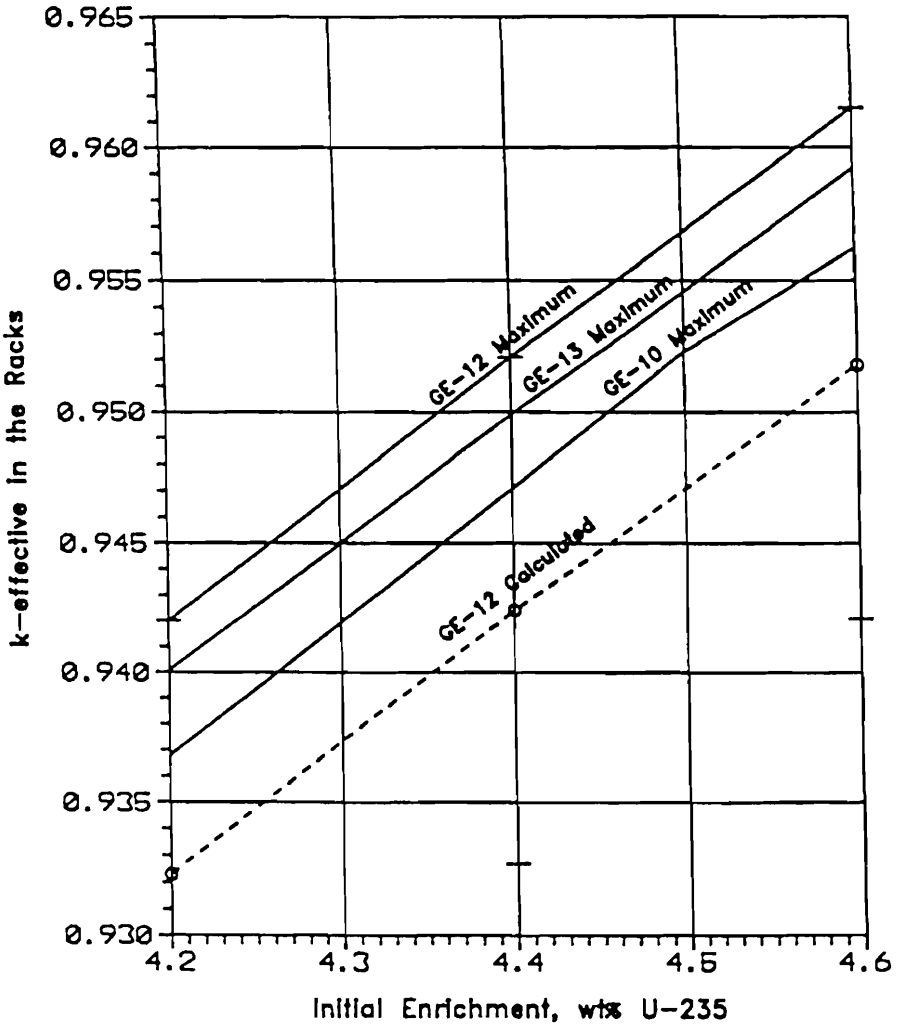

Fig. 1.2 Maximum k-effective in PaR Racks for Fuel of Various Average Enrichments and Types

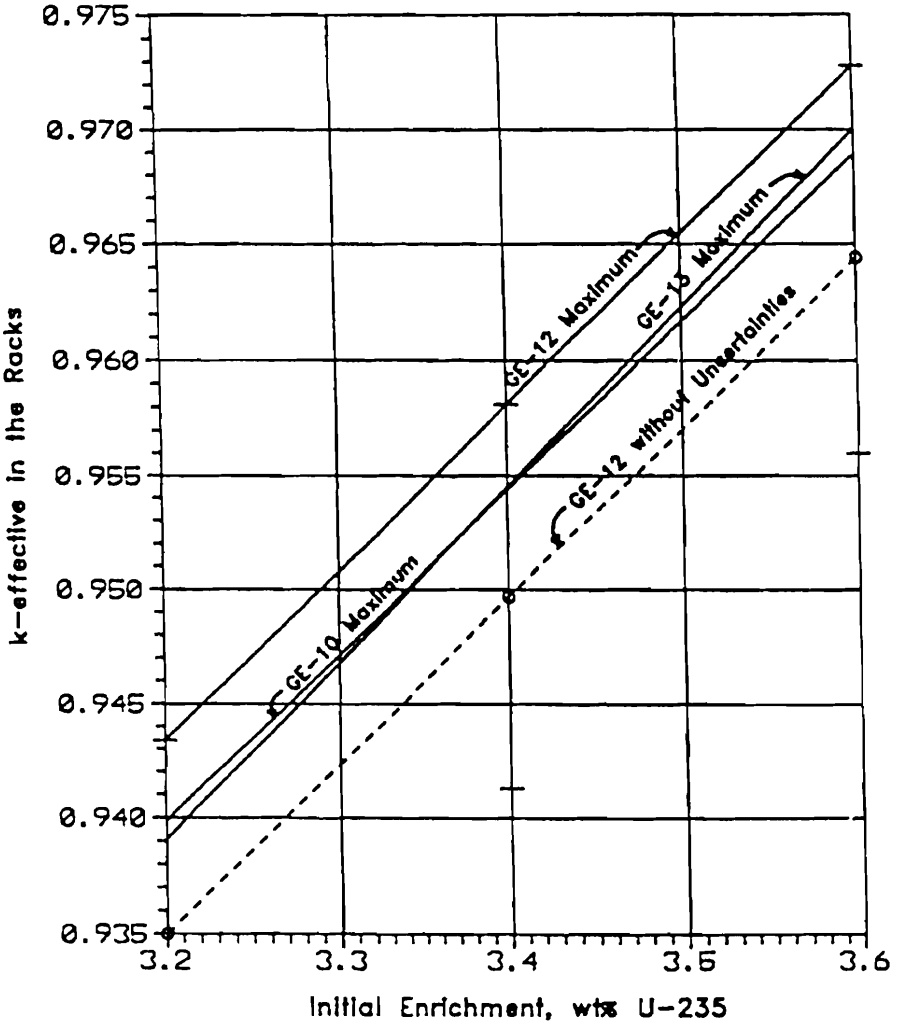

Fig. 1.3 Maximum k-effective in Holtec Racks for Fuel of Various Average Enrichments and Types

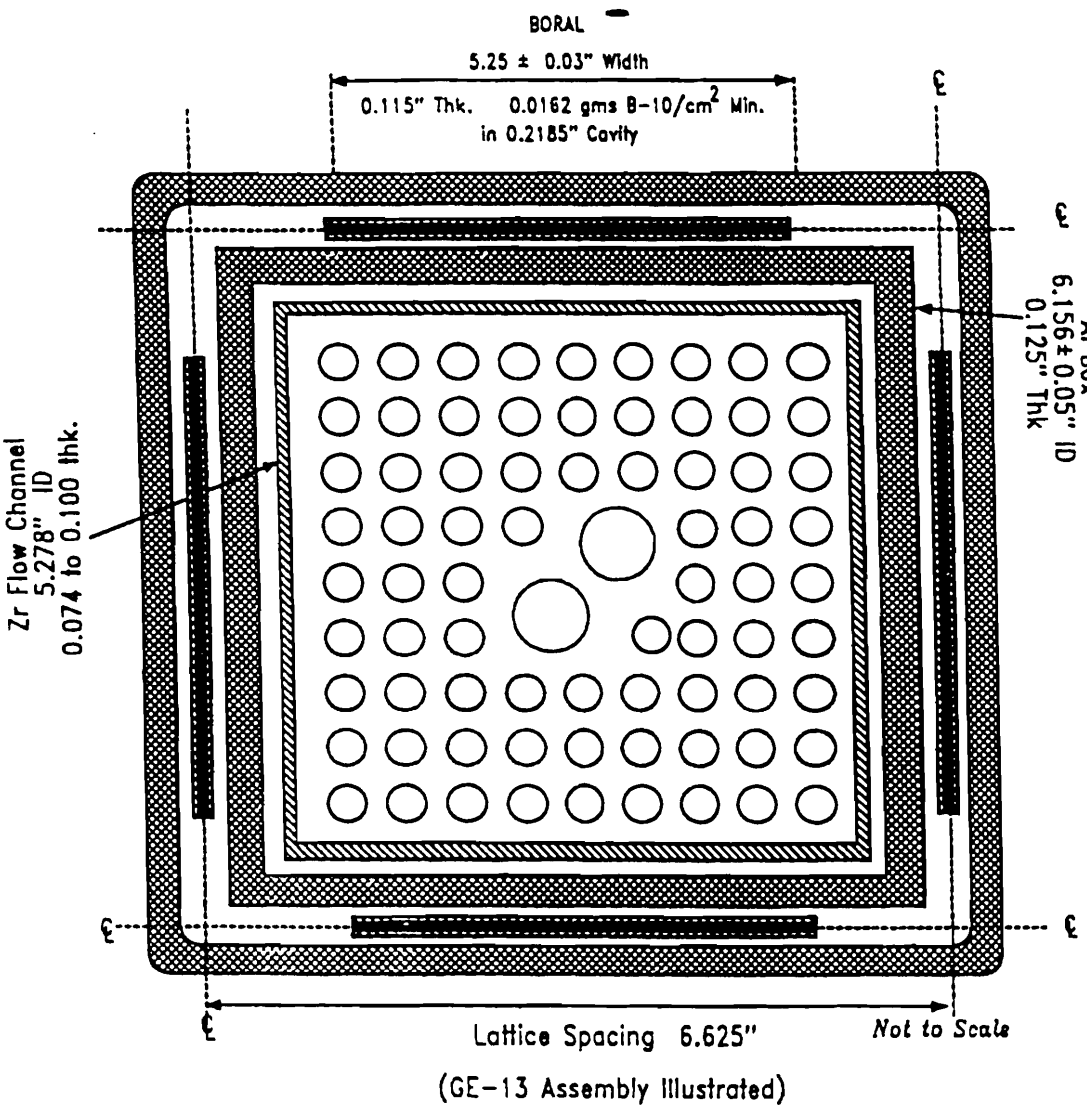

(GE-13 Assembly Illustrated)

Figure 2.1 Storage Cell Calculational Model for the Par Racks

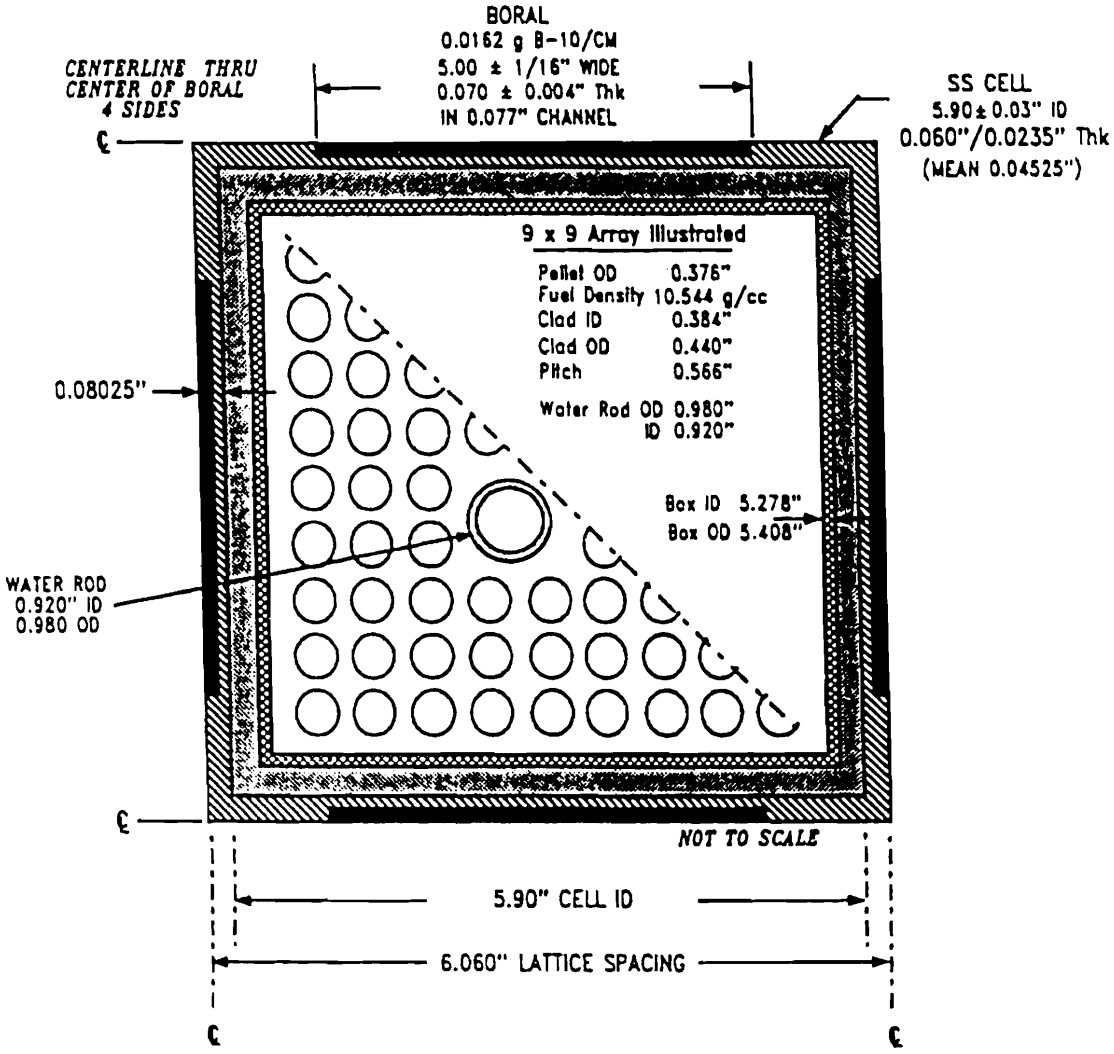

Fig. 2.2 Storage Cell Calculational Model for the Holtec Racks

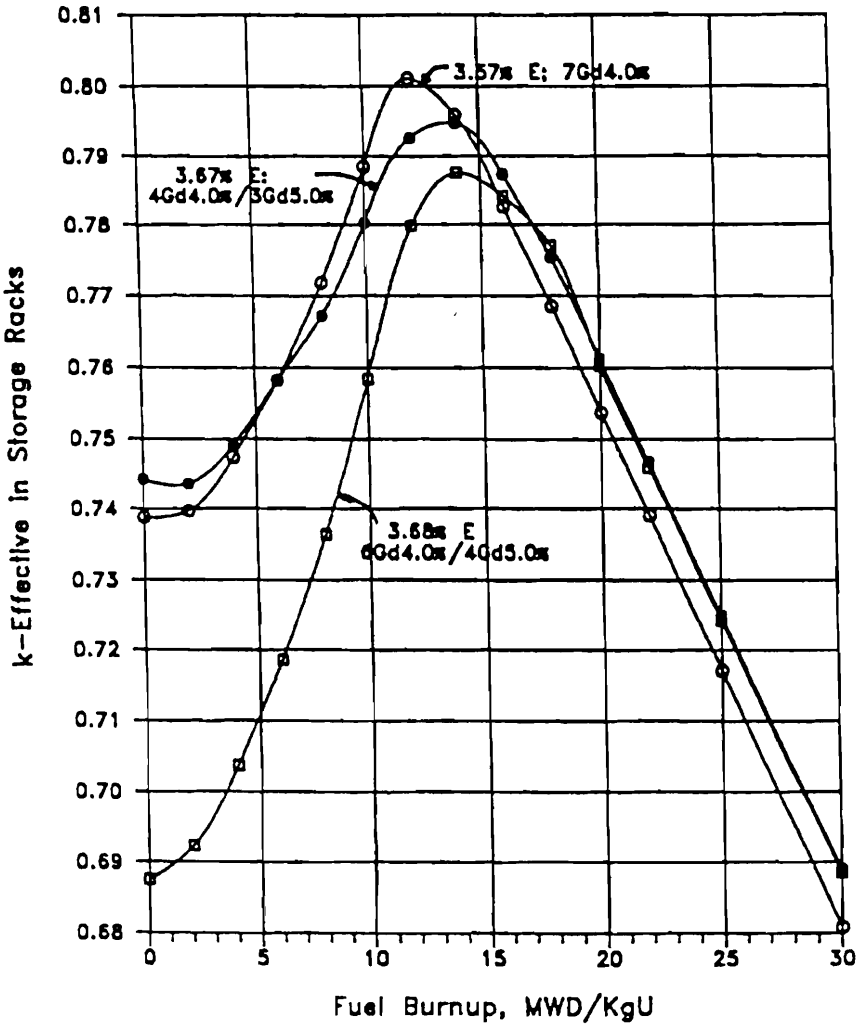

Fig. 5.1 Burnup Dependent Reactivity with Existing GE-10 Fuel in the PaR Storage Rack

Fig. 5.2

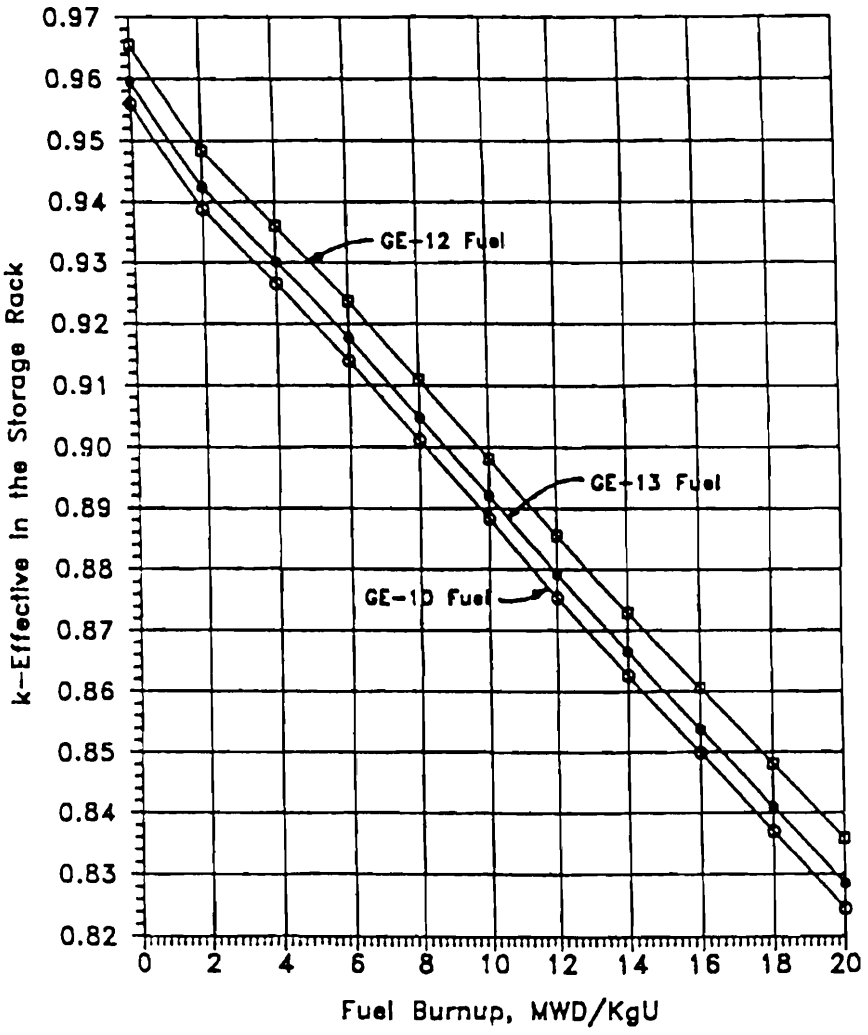

Fig. 5.3 Decrease in Reactivity with Burnup in PaR Racks for 4.6% Enriched Fuel without Gadolinia

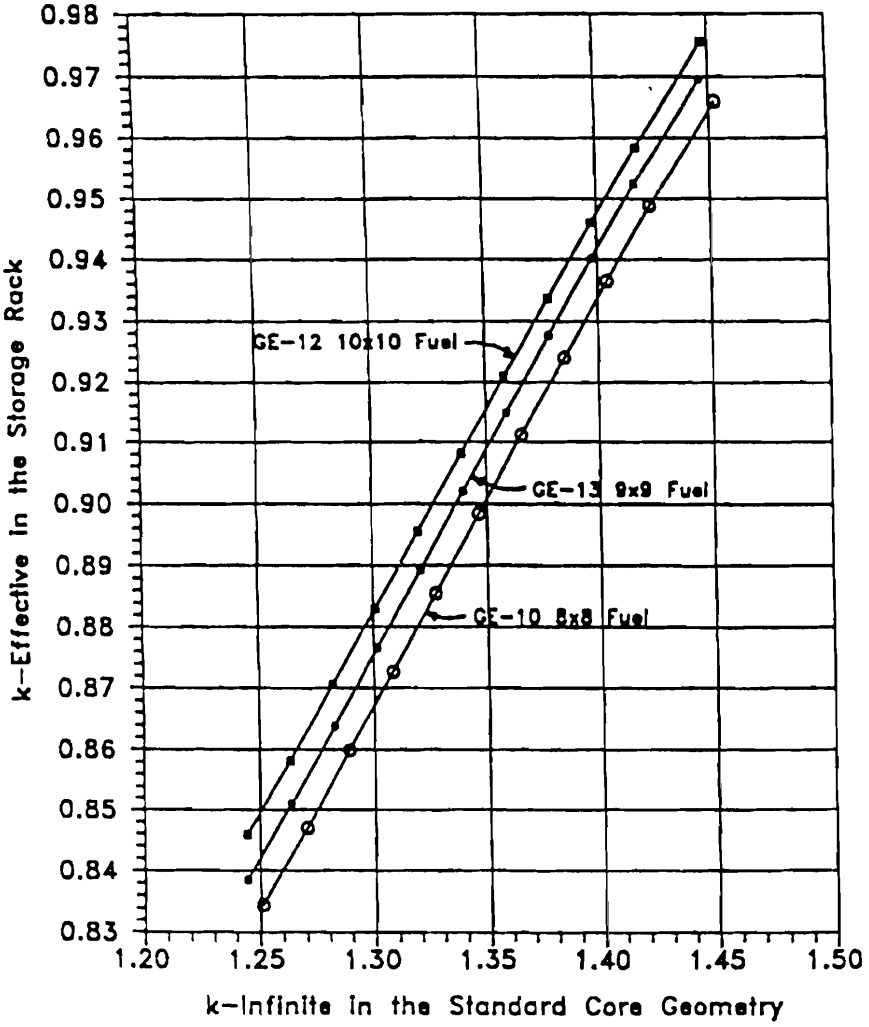

Fig. 5.4 Relationship Between Maximum k-effective in the PaR Storage Rack and the Standard Core k-Infinity (4.60% Enrichment)

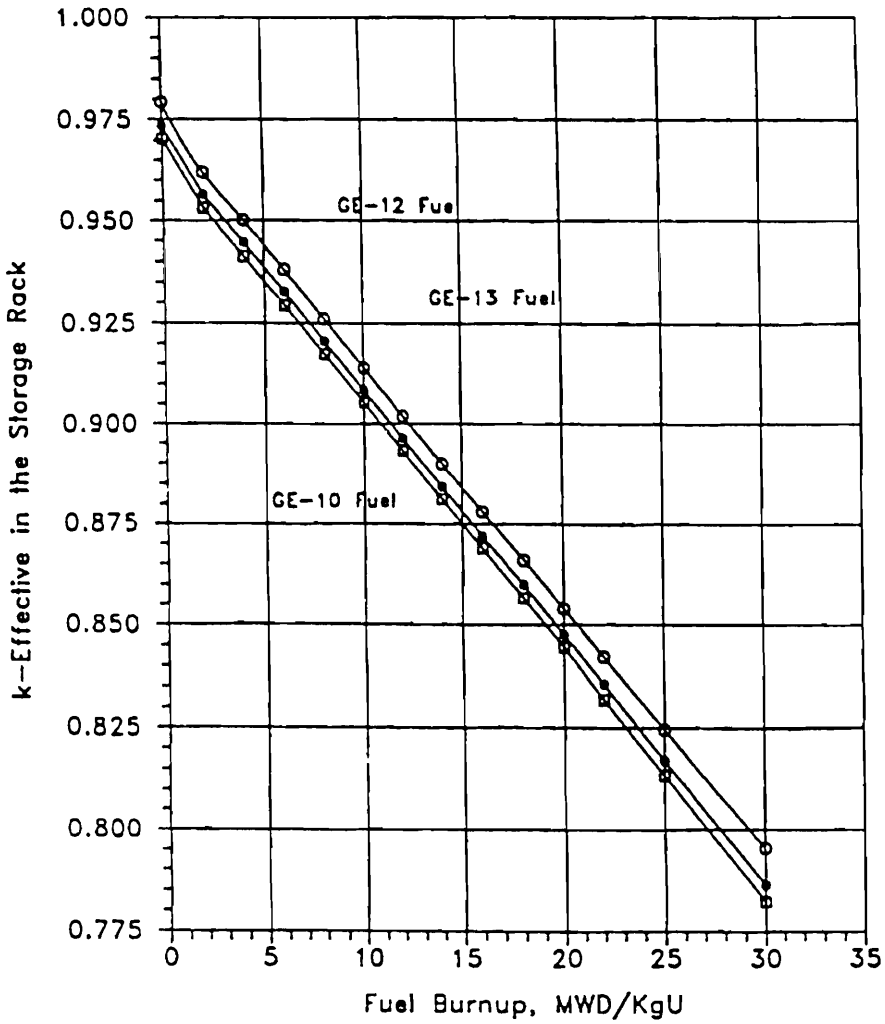

Fig. 5.5 Decrease in Reactivity with Burnup in PaR Racks for 4.95' Enriched Fuel Without Gadolinia

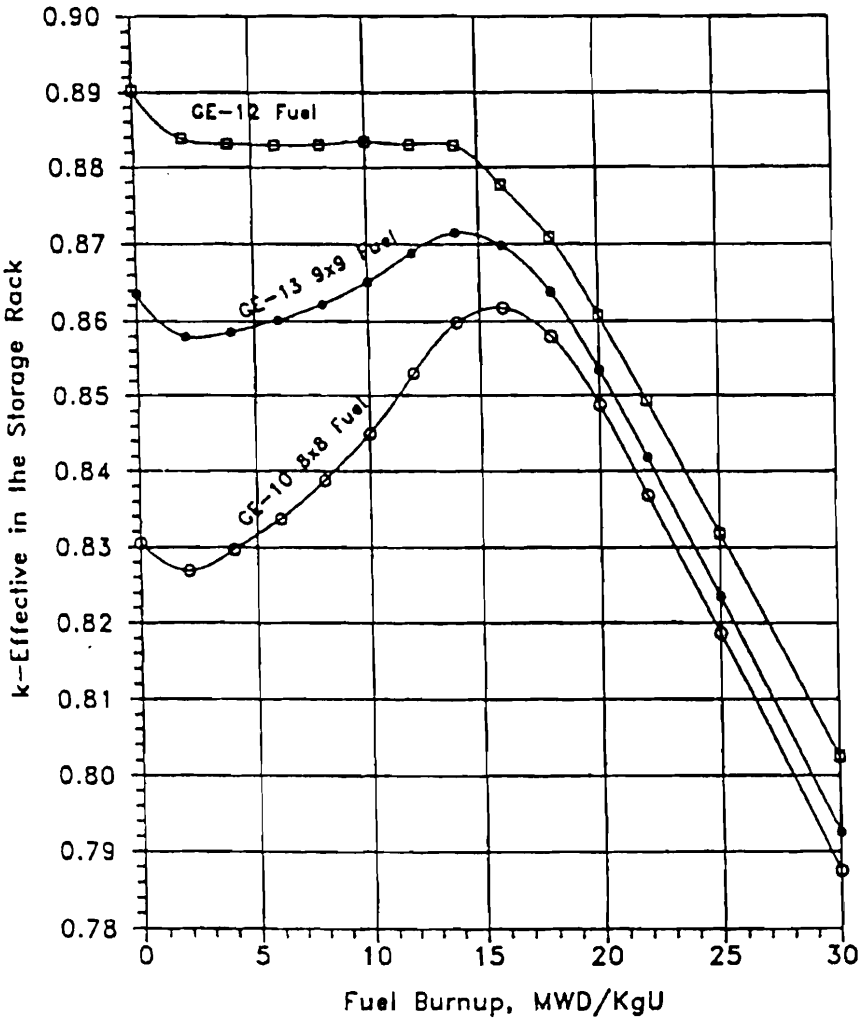

Fig. 5.6 Burnup Dependent Maximum Reactivity in the PaR Racks with 4.95' Enriched Fuel and 7-Gd-4.0'

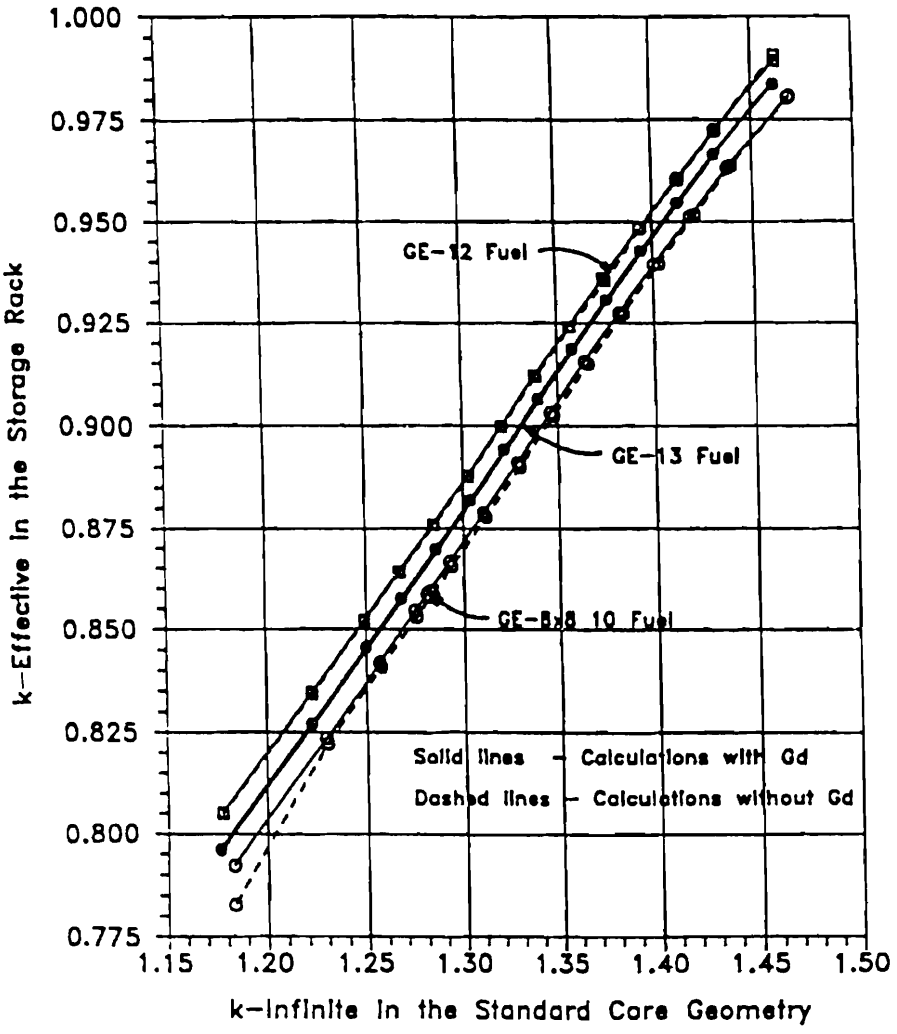

Fig. 5.7 Relationship Between Maximum k-effective in the PaR Storage Rack and the Standard Core k-Infinity (4.95% Enrichment)

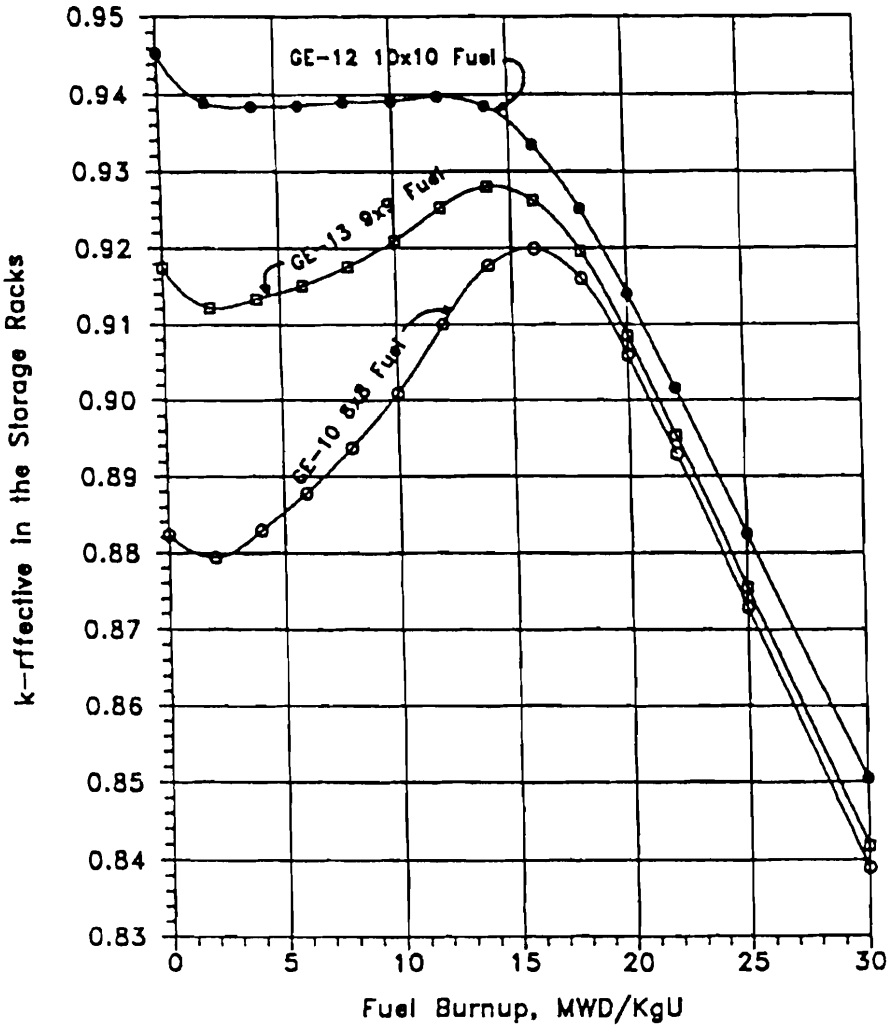

Fig. 5.8 Burnup Dependent Maximum Reactivity in the Holtec Racks with 4.95% Enriched Fuel and 7-Gd-4.0%

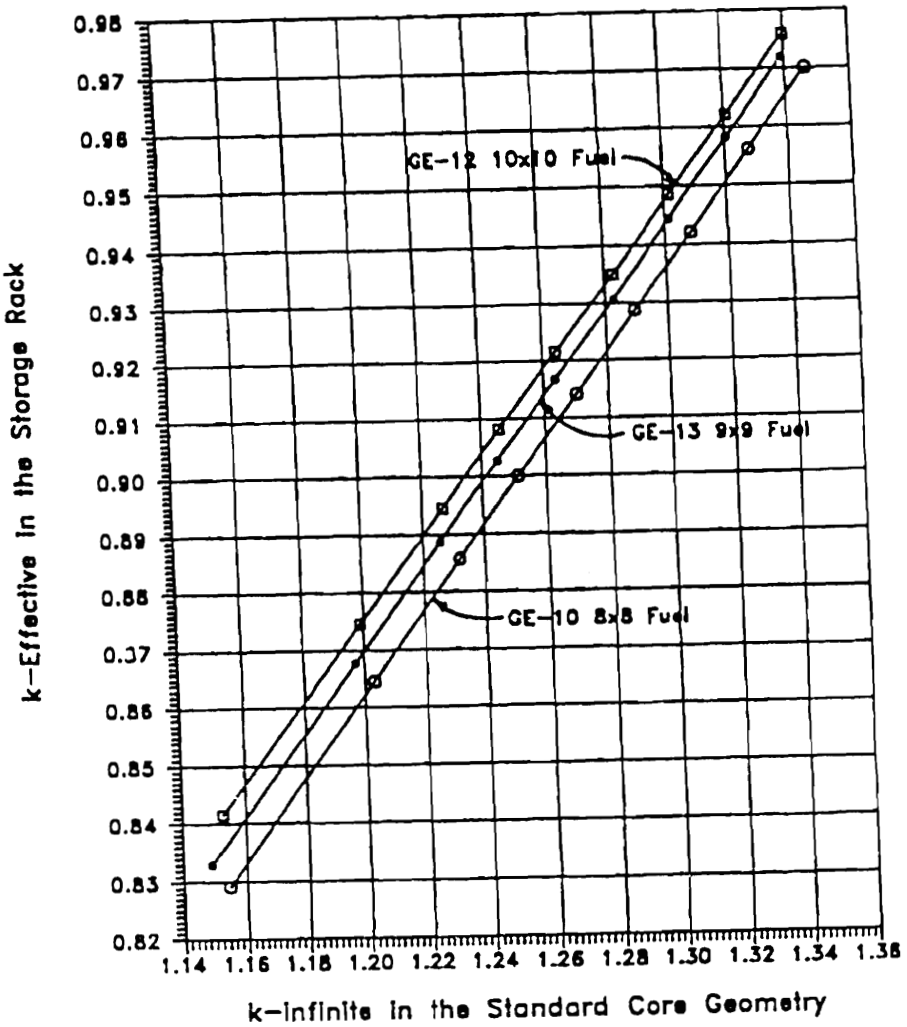

Fig. 5.9 Relationship Between Maximum k-effective in the Holtec Rack and the Standard Core k-Infinity (4.60% Enrichment)

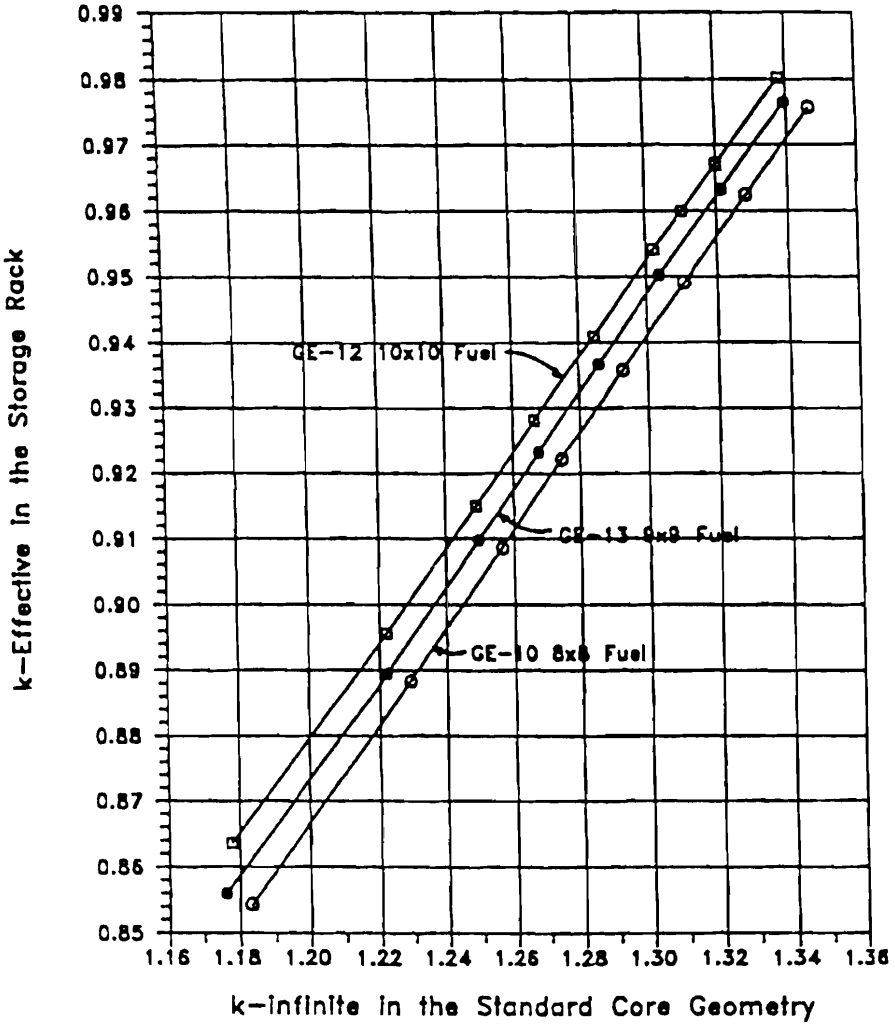

Fig. 5.10 Relationship Between Maximum k-effective in the Holtec Rack and the Standard Core k-Infinity (4.95% Enrichment)

APPENDIX A: BENCHMARK CALCULATIONS

A.1 INTRODUCTION AND SUMMARY

Benchmark calculations have been made on selected critical experiments, chosen, in so far as possible, to bound the range of variables in the rack designs. Two independent methods of analysis were used, differing in cross section libraries and in the treatment of the cross sections. MCNP [A.1] is a continuous energy Monte Carlo code and KENO5a [A.2] uses group-dependent cross sections. For the KENO5a analyses reported here, the 238-group library was chosen, processed through the NITAWL-II [A.2] program to create a working library and to account for resonance self-shielding in uranium-238 (Nordheim integral treatment). The 238 group library was chosen to avoid or minimize the errors[1] (trends) that have been reported (e.g., [A.3 through A.5]) for calculations with collapsed cross section sets.

In rack designs, the three most significant parameters affecting criticality are (1) the fuel enrichment, (2) the ^{10}B loading in the neutron absorber, and (3) the lattice spacing (or water-gap thickness if a flux-trap design is used). Other parameters, within the normal range of rack and fuel designs, have a smaller effect, but are also included in the analyses.

Table A.1 summarizes results of the benchmark calculations for all cases selected and analyzed, as referenced in the table. The effect of the major variables are discussed in subsequent sections below. It is important to note that there is obviously considerable overlap in parameters since it is not possible to vary a single parameter and maintain criticality; some other parameter or parameters must be concurrently varied to maintain criticality.

One possible way of representing the data is through a spectrum index that incorporates all of the variations in parameters. KENO5a computes and prints the "energy of the average lethargy causing fission". In MCNP, by utilizing the tally option with the identical 238-group energy structure as in KENO5a, the number of fissions in each group may be collected and the energy of the average lethargy causing fission determined (post-processing).

Figures A.1 and A.2 show the calculated k_{eff} for the benchmark critical experiments as a function of the "energy of the average lethargy causing fission" for MCNP and KENO5a, respectively (UO_2 fuel only). The scatter in the data (even for comparatively minor variation

---

[1] Small but observable trends (errors) have been reported for calculations with the 27-group and 44-group collapsed libraries. These errors are probably due to the use of a single collapsing spectrum when the spectrum should be different for the various cases analyzed, as evidenced by the spectrum indices.

in critical parameters) represents experimental error[2] in performing the critical experiments within each laboratory, as well as between the various testing laboratories. The B&W critical experiments show a larger experimental error than the PNL criticals. This would be expected since the B&W criticals encompass a greater range of critical parameters than the PNL criticals.

Linear regression analysis of the data in Figures A.1 and A.2 show that there are no trends, as evidenced by very low values of the correlation coefficient (0.13 for MCNP and 0.21 for KENO5a). The total bias (systematic error, or mean of the deviation from a k_{eff} of exactly 1.000) for the two methods of analysis are shown in the table below.

Calculational Bias of MCNP and KENO5a		
	Total	Truncated
MCNP	0.0019±0.0007	0.0025±0.0010
KENO5a	0.0040±0.0010	0.0042±0.0010

The values of bias shown in this table include both the bias derived directly from the calculated k_{eff} values in Table A.1, and a more conservative value derived by arbitrarily truncating to 1.000 any calculated value that exceeds 1.000. The bias and standard error of the bias were calculated by the following equations[3], with the standard error multiplied by the one-sided K-factor for 95% probability at the 95% confidence level from NBS Handbook 91 [A.18] (for the number of cases analyzed, the K-factor is ~2.08 or slightly more than 2).

$$\bar{k} = \frac{1}{n} \sum_{i}^{n} k_i \qquad \text{(A.1)}$$

---

2 A classical example of experimental error is the corrected enrichment in the PNL experiments, first as an addendum to the initial report and, secondly, by revised values in subsequent reports for the same fuel rods.

3 These equations may be found in any standard text on elementary statistics, for example, reference [A.6] (or the MCNP manual) and is the same methodology used in MCNP and in KENO5a.

$$\sigma_{\bar{k}}^2 = \frac{\sum_{i=1}^{n} k_i^2 - (\sum_{i=1}^{n} k_i)^2 / n}{n\,(n-1)} \qquad \text{(A.2)}$$

$$Bias = 1 - \bar{k} \pm K\,\sigma_{\bar{k}} \qquad \text{(A.3)}$$

where k_i are the calculated reactivities of n critical experiments; $\sigma_{\bar{k}}$ is the unbiased estimator of the standard deviation of the mean (also called the standard error of the bias (mean)); K is the one-sided multiplier for 95% probability at the 95% confidence level (NBS Handbook 91 [A.18]).

The larger of the systematic errors (truncated bias) were used to evaluate the maximum k_{eff} values for the rack designs. KENO5a has a slightly larger systematic error than MCNP, but both result in greater precision than published data [A.3 through A.5] would indicate for collapsed cross section sets in KENO5a (SCALE) calculations.

A.2 Effect of Enrichment

The benchmark critical experiments include those with enrichments ranging from 2.46% to 5.74% and therefore span the enrichment range for rack designs. Figures A.3 and A.4 show the calculated k_{eff} values (Table A.1) as a function of the fuel enrichment reported for the critical experiments. Linear regression analyses for these data confirms that there are no trends, as indicated by low values of the correlation coefficients (0.026 for MCNP and 0.379 for KENO5a). Thus, there are no corrections to the bias for the various enrichments.

As further confirmation of the absence of any trends with enrichment, a typical configuration was calculated with both MCNP and KENO5a for various enrichments. The cross-comparison of calculations with codes of comparable sophistication is suggested in Reg. Guide 3.41. Results of this comparison, shown in Table A.2 and Figure A.5, confirm no significant difference in the calculated values of k_{eff} for the two independent codes as evidenced by the 45° slope of the curve. Since it is very unlikely that two independent methods of analysis would be subject to the same error, this comparison is considered confirmation of the absence of an enrichment effect (trend) in the bias.

A.3 Effect of ^{10}B Loading

Several laboratories have performed critical experiments with a variety of thin absorber panels similar to the Boral panels in the rack designs. Of these critical experiments, those performed by B&W are the most representative of the rack designs. PNL has also made some measurements with absorber plates, but, with one exception (a flux-trap experiment), the reactivity worth of the absorbers in the PNL tests is very low and any significant errors that might exist in the treatment of strong thin absorbers could not be revealed.

Table A.3 lists the subset of experiments using thin neutron absorbers (from Table A.1) and shows the reactivity worth (Δk) of the absorber.[4]

No trends with reactivity worth of the absorber are evident, although based on the calculations shown in Table A.3, some of the B&W critical experiments seem to have an unusually large experimental errors. B&W made an effort to report some of their experimental errors. Other laboratories did not evaluate their experimental errors.

To further confirm the absence of a significant trend with ^{10}B concentration in the absorber, a cross-comparison was made with MCNP and KENO5a (as suggested in Reg. Guide 3.41). Results are shown in Figure A.6 and Table A.4 for a typical geometry. These data substantiate the absence of any error (trend) in either of the two codes for the conditions analyzed (data points fall on a 45° line, within an expected 95% probability limit.

A.4 Miscellaneous and Minor Parameters

A.4.1 Reflector Material and Spacings

PNL has performed a number of critical experiments with thick steel and lead reflectors.[5] Analysis of these critical experiments are listed in Table A.5 (subset of data in Table A.1). There appears to be a small tendency toward overprediction of k_{eff} at the lower spacing, although there are an insufficient number of data points in each series to allow a quantitative determination of any trends. The tendency toward overprediction at close spacing means that the rack calculations may be slightly more conservative than otherwise.

---

[4] The reactivity worth of the absorber panels was determined by repeating the calculation with the absorber analytically removed and calculating the incremental (Δk) change in reactivity due to the absorber.

[5] Parallel experiments with a depleted uranium reflector were also performed but not included in the present analysis since they are not pertinent to the Holtec rack design. A lead reflector is also not directly pertinent, but might be used in future designs.

A.4.2 Fuel Pellet Diameter and Lattice Pitch

The critical experiments selected for analysis cover a range of fuel pellet diameters form 0.311 to 0.444 inches, and lattice spacings from 0.476 to 1.00 inches. In the rack designs, the fuel pellet diameters range from 0.303 to 0.3805 inches O.D. (0.496 to 0.580 inch lattice spacing) for PWR fuel and from 0.3224 to 0.494 inches O.D. (0.488 to 0.740 inch lattice spacing) for BWR fuel. Thus, the critical experiments analyzed provide a reasonable representation of power reactor fuel. Based on the data in Table A.1, there does not appear to be any observable trend with either fuel pellet diameter or lattice pitch, at least over the range of the critical experiments applicable to rack designs.

A.4.3 Soluble Boron Concentration Effects

Various soluble boron concentrations were used in the B&W series of critical experiments and in one PNL experiment, with boron concentrations ranging up to 2550 ppm. Results of MCNP (and one KENO5a) calculations are shown in Table A. Analyses of the very high boron concentration experiments (>1300 ppm) show a tendency to slightly overpredict reactivity for the three experiments exceeding 1300 ppm. In turn, this would suggest that the evaluation of the racks with higher soluble boron concentrations could be slightly conservative.

A.5 MOX Fuel

The number of critical experiments with PuO_2 bearing fuel (MOX) is more limited than for UO_2 fuel.[6] However, a number of MOX critical experiments have been analyzed and the results are shown in Table A.7. Results of these analyses are generally above a k_{eff} of 1.00, indicating that when Pu is present, both MCNP and KENO5a overpredict the reactivity. This may indicate that calculation for MOX fuel will be expected to be conservative, especially with MCNP. It may be noted that for the larger lattice spacings, the KENO5a calculated reactivities are below 1.00, suggesting that a small trend may exist with KENO5a. It is also possible that the overprediction in k_{eff} for both codes may be due to a small inadequacy in the determination of the Pu-241 decay and Am-241 growth. This possibility is supported by the consistency in calculated k_{eff} over a wide range of the spectral index (energy of the average lethargy causing fission).

---

[6] Analyses of the MOX fuel critical experiments were not included in the evaluation of the calculational bias for MCNP and NITAWL-KENO5a.

A.6 References

[A.1] J.F. Briesmeister, Ed., "MCNP - A General Monte Carlo N-Particle Transport Co., Version 4A; Los Alamos National Laboratory, LA-12625-M (1993).

[A.2] SCALE 4.3, "A Modular Code System for Performing Standardized Computer Analyses for Licensing Evaluation", NUREG-0200 (ORNL-NUREG-CSD-2/U2/R5, Revision 5, Oak Ridge National Laboratory, September 1995.

[A.3] M.D. DeHart and S.M. Bowman, "Validation of the SCALE Broad Structure 44-G Group ENDF/B-Y Cross-Section Library for Use in Criticality Safety Analyses", NUREG/CR-6102 (ORNL/TM-12460) Oak Ridge National Laboratory, September 1994.

[A.4] W.C. Jordan et al., "Validation of KENOV.a", CSD/TM-238, Martin Marietta Energy Systems, Inc., Oak Ridge National Laboratory, December 198

[A.5] O.W. Hermann et al., "Validation of the Scale System for PWR Spent Fuel Isotopic Composition Analysis", ORNL-TM-12667, Oak Ridge National Laboratory, undated.

[A.6] R.J. Larsen and M.L. Marx, An Introduction to Mathematical Statistics and its Applications, Prentice-Hall, 198

[A.7] M.N. Baldwin et al., Critical Experiments Supporting close Proximity Water Storage of Power Reactor Fuel, BAW-1484-7, Babcock and Wilcox Company, July 1979.

[A.8] G.S. Hoovier et al., Critical Experiments Supporting Underwater Storage of Tightly Packed Configurations of Spent Fuel Pins, BAW-1645-4, Babcock & Wilcox Company, November 1991.

[A.9] L.W. Newman et al., Urania Gadolinia: Nuclear Model Development and Critical Experiment Benchmark, BAW-1810, Babcock and Wilcox Company, April 1984.

[A.10] J.C. Manaranche et al., "Dissolution and Storage Experimental Program with 4.75% Enriched Uranium-Oxide Rods," Trans. Am. Nucl. Soc. 33: 362-364 (1979).

[A.11] S.R. Bierman and E.D. Clayton, Criticality Experiments with Subcritical Clusters of 2.35 wt % and 4.31 wt % ^{235}U Enriched UO^2 Rods in Water with Steel Reflecting Walls, PNL-3602, Battelle Pacific Northwest Laboratory, April 1981.

[A.12] S.R. Bierman et al., Criticality Experiments with Subcritical Clusters of 2.35 Wt% and 4.31 Wt% ^{235}U Enriched UO^2 Rods in Water with Uranium or Lead Reflecting Walls, PNL-3926, Battelle Pacific Northwest Laboratory, December, 1981.

[A.13] S.R. Bierman et al., Critical Separation Between Subcritical Clusters of 4.31 Wt % ^{235}U Enriched UO^2 Rods in Water with Fixed Neutron Poisons, PNL-2428, Battelle Pacific Northwest Laboratory, October 1977.

[A.14] S.R. Bierman, Criticality Experiments with Neutron Flux Traps Containing Voids, PNL-7167, Battelle Pacific Northwest Laboratory, April 1990.

[A.15] B.M. Durst et al., Critical Experiments with 4.31 wt % ^{235}U Enriched UO_2 Rods in Highly Borated Water Lattices, PNL-4267, Battelle Pacific Northwest Laboratory, August 1982.

[A.16] S.R. Bierman, Criticality Experiments with Fast Test Reactor Fuel Pins in Organic Moderator, PNL-5803, Battelle Pacific Northwest Laboratory, December 198

[A.17] E.G. Taylor et al., Saxton Plutonium Program Critical Experiments for the Saxton Partial Plutonium core, WCAP-3383-54, Westinghouse Electric Corp., Atomic Power Division, December 1965.

[A.18] M.G. Natrella, Experimental Statistics, National Bureau of Standards, Handbook 91, August 1963.

Table A.1

Summary of Criticality Benchmark Calculations

	Reference	Identification	Enrich.	k_{∞} Calculated		Energy of Ave Lethargy of Fission	
				MCNP	KENO5a	MCNP	KENO5a
1	B&W-1484 (6.A.7)	Core I	2.46	0.9964 ± 0.0010	0.9898 ± 0.0006	0.1759	0.1753
2	B&W-1484 (6.A.7)	Core II	2.46	1.0008 ± 0.0011	1.00154 ± 0.0005	0.2553	0.2446
3	B&W-1484 (6.A.7)	Core III	2.46	1.0010 ± 0.0012	1.0005 ± 0.0005	0.1999	0.1939
4	B&W-1484 (6.A.7)	Core IX	2.46	0.9956 ± 0.0012	0.9901 ± 0.0006	0.1422	0.1426
5	B&W-1484 (6.A.7)	Core X	2.46	0.9980 ± 0.0014	0.9922 ± 0.0006	0.1513	0.1499
6	B&W-1484 (6.A.7)	Core XI	2.46	0.9978 ± 0.0012	1.0005 ± 0.0005	0.2031	0.1947
7	B&W-1484 (6.A.7)	Core XII	2.46	0.9988 ± 0.0011	0.9978 ± 0.0006	0.1718	0.1662
8	B&W-1484 (6.A.7)	Core XIII	2.46	1.0020 ± 0.0010	0.9952 ± 0.0006	0.1988	0.1965
9	B&W-1484 (6.A.7)	Cote XIV	2.46	0.9953 ± 0.0011	0.9928 ± 0.0006	0.2022	0.1986
10	B&W-1484 (6.A.7)	Core XV	2.46	0.9910 ± 0.0011	0.9909 ± 0.0006	0.2092	0.2014
11	B&W-1484 (6.A.7)	Core XVI	2.46	0.9935 ± 0.0010	0.9889 ± 0.0006	0.1757	0.1713
12	B&W-1484 (6.A.7)	Core XVII	2.46	0.9962 ± 0.0012	0.9942 ± 0.0005	0.2083	0.2021

Table A.1 (Continued)

	Reference	Identification	Enrich.	k_{∞} Calculated		Energy of Ave Lethargy of Fission	
				MCNP	KENO5a	MCNP	KENO5a
13	B&W-1484 (A.7)	Core XVIII	2.46	1.0036 ± 0.0012	0.9931 ± 0.0006	0.1705	0.1708
14	B&W-1484 (A.7)	Core XIX	2.46	0.9961 ± 0.0012	0.9971 ± 0.0005	0.2103	0.2011
15	B&W-1484 (A.7)	Core XX	2.46	1.0008± 0.0011	0.9932 ± 0.0006	0.1724	0.1701
16	B&W-1484 (A.7)	Core XXI	2.46	0.9994 ± 0.0010	0.9918 ± 0.0006	0.1544	0.1536
17	B&W-1645 (A.7)	S-type fuel, w/886 ppm B	2.46	0.9970 ± 0.0010	0.9924 ± 0.0006	1.4475	1.4680
18	B&W-1645 (A.8)	S-type Fuel, w/746 ppm B	2.46	0.9990 ± 0.0010	0.9913 ± 0.0006	1.5463	1.5660
19	B&W-1645 (A.8)	SO-type Fuel, w/1156 ppm B	2.46	0.9972± 0.0009	0.9949 ± 0.0005	0.4241	0.4331
20	B&W-1810 (A.8)	Case 1 1337 ppm B	2.46	1.0023 ± 0.0010	NC	0.1531	NC
21	B&W-1810 (A.9)	Case 12 1899 ppm B	2.46/4.02	1.0060 ± 0.0009	NC	0.4493	NC
22	French (A.10)	Water Moderator 0 gap	4.75	0.9966 ± 0.0013	NC	0.2172	NC
23	French (A.10)	Water Moderator 2.5 cm gap	4.75	0.9952 ± 0.0012	NC	0.1778	NC
24	French (A.10)	Water Moderator 5 cm gap	4.75	0.9943 ± 0.0010	NC	0.1677	NC

Table A.1 (Continued)

	Reference	Identification	Enrich.	k_{∞} Calculated		Energy of Ave Lethargy of Fission	
				MCNP	KENO5a	MCNP	KENO5a
25	French (A.10)	Water Moderator 10 cm gap	4.75	0.9979 ± 0.0010	NC	0.1736	NC
26	PNL-3602 (A.11)	Steel Reflector, 0 separation	2.35	NC	1.0004 ± 0.0006	NC	0.1018
27	PNL-3602 (A.11)	Steel Reflector, 1.321 cm sepn.	2.35	0.9980 ± 0.0009	0.9992 ± 0.0006	0.1000	0.0909
28	PNL-3602 (A.11)	Steel Reflector, 2.616 cm sepn.	2.35	0.9968 ± 0.0009	0.9964 ± 0.0006	0.0981	0.0975
29	PNL-3602 (A.11)	Steel Reflector, 3.912 cm sepn.	2.35	0.9974 ± 0.0010	0.9980 ± 0.0006	0.0976	0.0970
30	PNL-3602 (A.11)	Steel Reflector, Infinite sepn.	2.35	0.9962 ± 0.0008	0.9939 ± 0.0006	0.0973	0.0968
31	PNL-3602 (A.11)	Steel Relector, 0 cm sepn.	2.35	NC	1.0003 ± 0.0007	NC	0.3282
32	PNL-3602 (A.11)	Steel Reflector, 1.321 cm sepn.	2.35	0.9997 ± 0.0010	1.0012 ± 0.0007	0.3016	0.3039
33	PNL-3602 (A.11)	Steel Reflector, 2.616 cm sepn.	4.306	0.9994 ± 0.0012	0.9974 ± 0.0007	0.2911	0.2927
34	PNL-3602 (A.11)	Steel Reflector, 5.405 cm sepn.	4.306	0.9969 ± 0.0011	0.9951 ± 0.0007	0.2828	0.2860
35	PNL-3602 (A.11)	Steel Reflector, Infinite sepn.	4.306	0.9910 ± 0.0020	0.9947 ± 0.0007	0.2851	0.2864
36	PNL-3926 (A.12)	Steel Reflector, with Boral Sheets	4.306	0.9941 ± 0.0011	0.9970 ± 0.0007	0.3135	0.3150

Table A.1 (Continued)

	Reference	Identification	Enrich.	k_{∞} Calculated		Energy of Ave Letharry of Fission	
				MCNP	KENO5a	MCNP	KENO5a
37	PNL-3926 (A.12)	Lead Reflector, 0 cm sepn.	4.306	NC	1.0003 ± 0.0007	NC	0.3159
38	PNL-3926 (A.12)	Lead Reflector, 0.55 cm sepn.	4.306	1.0025 ± 0.0011	0.9997 ± 0.0007	0.3030	0.3044
39	PNL-3926 (A.12)	Lead Reflector, 1.956 cm sepn.	4.306	1.0000 ± 0.0012	0.9985 ± 0.0007	0.2883	0.2930
40	PNL-3926 (A.12)	Lead Reflector, 5.405 cm sepn.	4.306	0.9971 ± 0.0012	0.9946 ± 0.0007	0.2831	0.2854
41	PNL-2615 (A.13)	Experiment 004/032 - no absorber	4.306	0.9925 ± 0.0012	0.9950 ± 0.0007	0.1155	0.1159
42	PNL-2615 (A.13)	Experiment 030 - Zr plates	4.306	NC	0.9971 ± 0.0007	NC	0.1154
43	PNL-2615 (A.13)	Experiment 013 - Steel plates	4.306	NC	0.9965 ± 0.0007	NC	0.1164
44	PNL-2615 (A.13)	Experiment 014 - Steel Plates	4.306	NC	0.9972 ± 0.0007	NC	0.1164
45	PNL-2615 (A.13)	Exp. 009 1.05% Boron-Steel plates	4.306	0.9982 ± 0.0010	0.9981 ± 0.0007	0.1172	0.1162
46	PNL-2615 (A.13)	Exp. 012 1.62% Boron-Steel plates	4.306	0.9996 ± 0.0012	0.9982 ± 0.0007	0.1161	0.1173
47	PNL-2615 (A.13)	Exp. 031 - Boral plates	4.306	0.9994 ± 0.0012	0.9969 ± 0.0007	0.1165	0.1171
48	PNL-7167 (A.14)	Experiment 214R - with flux trap	4.306	0.9991 ± 0.0011	0.9956 ± 0.0007	0.3722	0.3812

Table A.1 (Continued)

	Reference	Identification	Enrich.	k_{∞} Calculated		Energy of Ave Lethargy of Fission	
				MCNP	KENO5a	MCNP	KENO5a
49	PNL-7167 (A.14)	Experiment 214V3 - with flux trap	4.306	0.9969 ± 0.0011	0.9963 ± 0.0007	0.3742	0.3826
50	PNL-4267 (A.15)	Case 173 - 0 ppm B	4.306	0.9974 ± 0.0012	NC	0.2893	NC
51	PNL-4267 (A.15)	Case 177 - 2550 ppm B	4.306	1.0057 ± 0.0010	NC	0.5509	NC
52	PNL-5803 (A.16)	MOX Fuel - Type 3.2 Exp. 21	20% Pu	1.0041 ± 0.0011	1.0046 ± 0.0006	0.9171	0.8868
53	PNL-5803 (A.16)	MOX Fuel - Type 3.2 Exp. 43	20% Pu	1.0058 ± 0.0012	1.0036 ± 0.0006	0.2968	0.2944
54	PNL-5803 (A.16)	MOX Fuel - Type 3.2 Exp. 13	20% Pu	1.0083 ± 0.0011	0.9989 ± 0.0006	0.1665	0.1706
55	PNL-5803 (A.16)	MOX Fuel - Type 3.2 Exp. 32	20% Pu	1.0079 ± 0.0011	0.9966 ± 0.0006	0.1139	0.1165
56	WCAP-3385 (A.17)	Saxton Case 52 PuO2 0.52" pitch	6.6% Pu	0.9996 ± 0.0011	1.0005 ± 0.0006	0.8665	0.8417
57	WCAP-3385 (A.17)	Saxton Case 52 U 0.52" pitch	5.74	1.0000 ± 0.0010	0.9956 ± 0.0007	0.4476	0.4580
58	WCAP-3385 (A.17)	Saxton Case 56 PuO2 0.56" pitch	6.6% Pu	1.0036 ± 0.0011	1.0047 ± 0.0006	0.5289	0.5197
59	WCAP-3385 (A.17)	Saxton Case 56 borated PuO2	6.6% Pu	1.0008 ± 0.0010	NC	0.6389	NC
60	WCAP-3385 (A.17)	Saxton Case 56 U 0.56" pitch	5.74	0.9994 ± 0.0011	NC	0.2923	NC

Table A.1 (Continued)

	Reference	Identification	Enrich.	k_∞ Calculated		Energy of Ave Lethargy of Fission	
				MCNP	KENO5a	MCNP	KENO5a
61	WCAP-3385 (A.17)	Saxton Case 79 PuO2 0..79" pitch	6.6% Pu	1.0063 ± 0.0011	1.0133 ± 0.0006	0.1520	0.1555
62	WCAP-3385 (A.17)	Saxton Case 79 U 0..79" pitch	5.74	1.0039 ± 0.0011	1.0008 ± 0.0006	0.1036	0.1047

Table A.2

COMPARISON OF MCNP AND KENO5a CALCULATED REACTIVITIES[7] FOR VARIOUS ENRICHMENTS

Enrichment	$k_{eff} \pm 1\sigma$	
	MCNP	KENO5a
3.0	0.8465 ± 0.0011	0.8478 ± 0.0004
3.5	0.8820 ± 0.0011	0.8841 ± 0.0004
3.75	0.9019 ± 0.0011	0.8987 ± 0.0004
4.0	0.9132 ± 0.0010	0.9140 ± 0.0004
4.2	0.9276 ± 0.0011	0.9237 ± 0.0004
4.5	0.9400 ± 0.0011	0.9388 ± 0.0004

[7] Based on the MPC-68 with the GE 8x8R.

Table A.3

MCNP CALCULATED REACTIVITIES FOR
CRITICAL EXPERIMENTS WITH NEUTRON ABSORBERS

Ref.	Experiment		Δk Worth of Absorber	k_{eff} Calculated	Energy of Average Lethargy of Fission
A.13	PNL-2615	Boral Sheet	0.0139	0.9994±0.0012	0.1165
A.7	B&W-1484	Core XX	0.0165	1.0008±0.0011	0.1724
A.13	PNL-2615	1.62% Boron-steel	0.0165	0.9996±0.0012	0.1161
A.7	B&W-1484	Core XIX	0.0202	0.9961±0.0012	0.2103
A.7	B&W-1484	Core XXI	0.0243	0.9994±0.0012	0.1544
A.7	B&W-1484	Core XVII	0.0519	0.9962±0.0012	0.2083
A.11	PNL-3602	Boral Sheet	0.0708	0.9941±0.0011	0.3135
A.7	B&W-1484	Core XV	0.0786	0.9910±0.0011	0.2092
A.7	B&W-1484	Core XVI	0.0845	0.9935±0.0010	0.1757
A.7	B&W-1484	Core XIV	0.1575	0.9953±0.0011	0.2022
A.7	B&W-1484	Core XIII	0.1738	1.0020±0.0011	0.1988
A.14	PNL-7167	Expt 214R flux trap	0.1931	0.9991±0.0011	0.3722

Table A.4

COMPARISON OF MCNP AND KENO5a
CALCULATED REACTIVITIES[1] FOR VARIOUS ^{10}B LOADINGS

^{10}B, g/cm^2	$k_{eff} \pm 1\sigma$	
	MCNP	KENO5a
0.005	1.0381 ± 0.0012	1.0340 ± 0.0004
0.010	0.9960 ± 0.0010	0.9941 ± 0.0004
0.015	0.9727 ± 0.0009	0.9713 ± 0.0004
0.020	0.9541 ± 0.0012	0.9560 ± 0.0004
0.025	0.9433 ± 0.0011	0.9428 ± 0.0004
0.03	0.9325 ± 0.0011	0.9338 ± 0.0004
0.035	0.9234 ± 0.0011	0.9251 ± 0.0004
0.04	0.9173 ± 0.0011	0.9179 ± 0.0004

[1] Based on 4.5% enrichment GE 8x8R in the MPC-68 cask.

Table A.5

CALCULATIONS FOR CRITICAL EXPERIMENTS WITH THICK LEAD AND STEEL REFLECTORS[9]

Ref.	Case	E, wt%	Separation, cm	MCNP k_{eff}	KENO5a k_{eff}
A.11	Steel Reflector	2.35	1.321	0.9980±0.0009	0.9992±0.0006
		2.35	2.616	0.9968±0.0009	0.9964±0.0006
		2.35	3.912	0.9974±0.0010	0.9980±0.0006
		2.35	∞	0.9962±0.0008	0.9939±0.0006
A.11	Steel Reflector	4.306	1.321	0.9997±0.0010	1.0012±0.0007
		4.306	2.616	0.9994±0.0012	0.9974±0.0007
		4.306	3.405	0.9969±0.0011	0.9951±0.0007
		4.306	∞	0.9910±0.0020	0.9947±0.0007
A.12	Lead Reflector	4.306	0.55	1.0025±0.0011	0.9997±0.0007
		4.306	1.956	1.0000±0.0012	0.9985±0.0007
		4.306	5.405	0.9971±0.0012	0.9946±0.0007

[9] Arranged in order of increasing reflector-fuel spacing.

Table A.6

CALCULATIONS FOR CRITICAL EXPERIMENTS WITH VARIOUS SOLUBLE BORON CONCENTRATIONS

Reference	Experiment	Boron Concentration, ppm	Calculated k_{eff}	
			MCNP	KENO5a
A.9	B&W-1810	1337	1.0023 ± 0.0010	-
A.9	B&W-1810	1899	1.0060 ± 0.0009	-
A.8	B&W-1645	886	0.9970 ± 0.0010	0.9924 ± 0.0006
A.15	PNL-4267	0	0.9974 ± 0.0012	-
A.15	PNL-4267	2550	1.0057 ± 0.0010	-

Table A.7

CALCULATIONS FOR CRITICAL EXPERIMENTS WITH MOX FUEL

Reference	Case[10]	MCNP		KENO	
		k_{eff}	EALF[11]	k_{eff}	EALF[11]
PNL-5803 [A.16]	MOX Fuel - Exp. No. 21	1.0041±0.0011	0.9171	1.0046±0.0006	0.8868
	MOX Fuel - Exp. No. 43	1.0058±0.0012	0.2968	1.0036±0.0006	0.2944
	MOX Fuel - Exp. No. 13	1.0083±0.0011	0.1665	0.9989±0.0006	0.1706
	MOX Fuel - Exp. No. 32	1.0079±0.0011	0.1139	0.9966±0.0006	0.1165
WCAP-3385 [A.17]	Saxton ● 0.52" pitch	0.9996±0.0011	0.8665	1.0005±0.0006	0.8417
	Saxton ● 0.56" pitch	1.0036±0.0011	0.5289	1.0047±0.0006	0.5197
	Saxton ● 0.56" pitch borated	1.0008±0.0010	0.6389	NC	NC
	Saxton ● 0.79" pitch	1.0063±0.0011	0.1520	1.0133±0.0006	0.1555

10 Arranged in order of increasing lattice spacing.

11 EALF is the energy of the average lethargy causing fission.

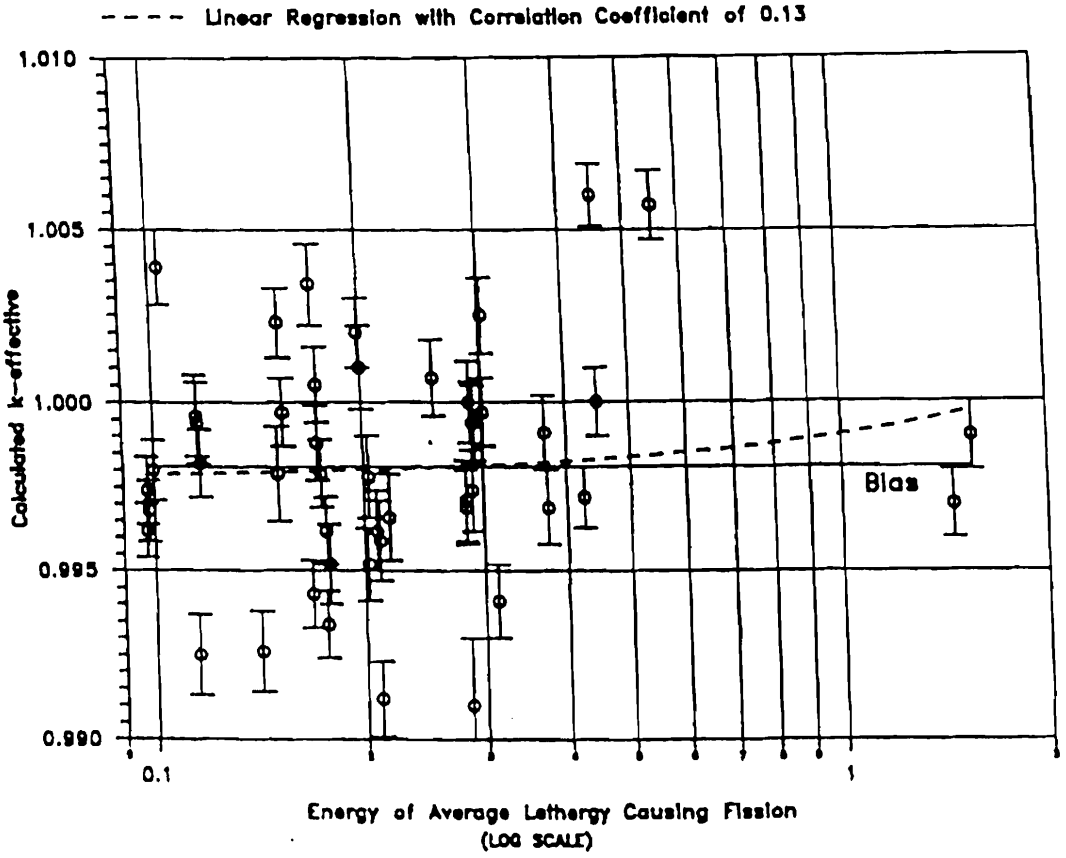

FIGURE A.1 MCNP CALCULATED k-eff VALUES for VARIOUS VALUES OF THE SPECTRAL INDEX

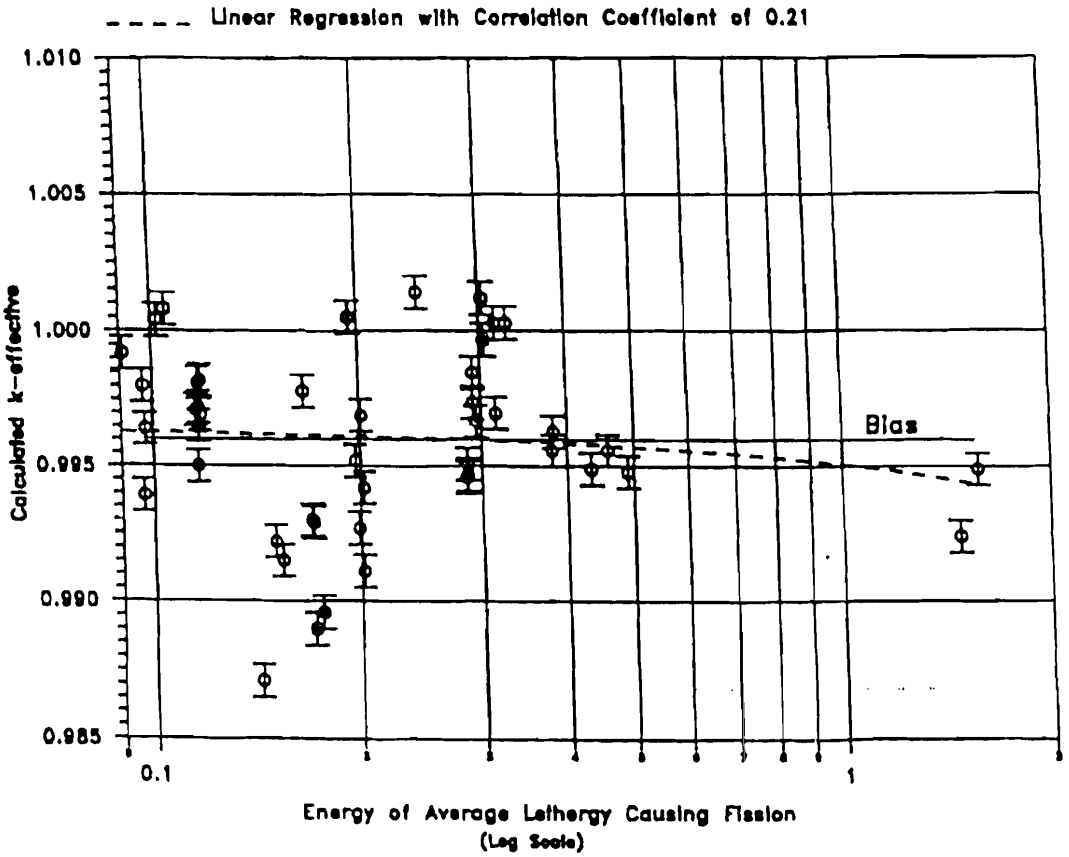

FIGURE A.2 KENO5a CALCULATED k-eff VALUES FOR VARIOUS VALUES OF THE SPECTRAL INDEX

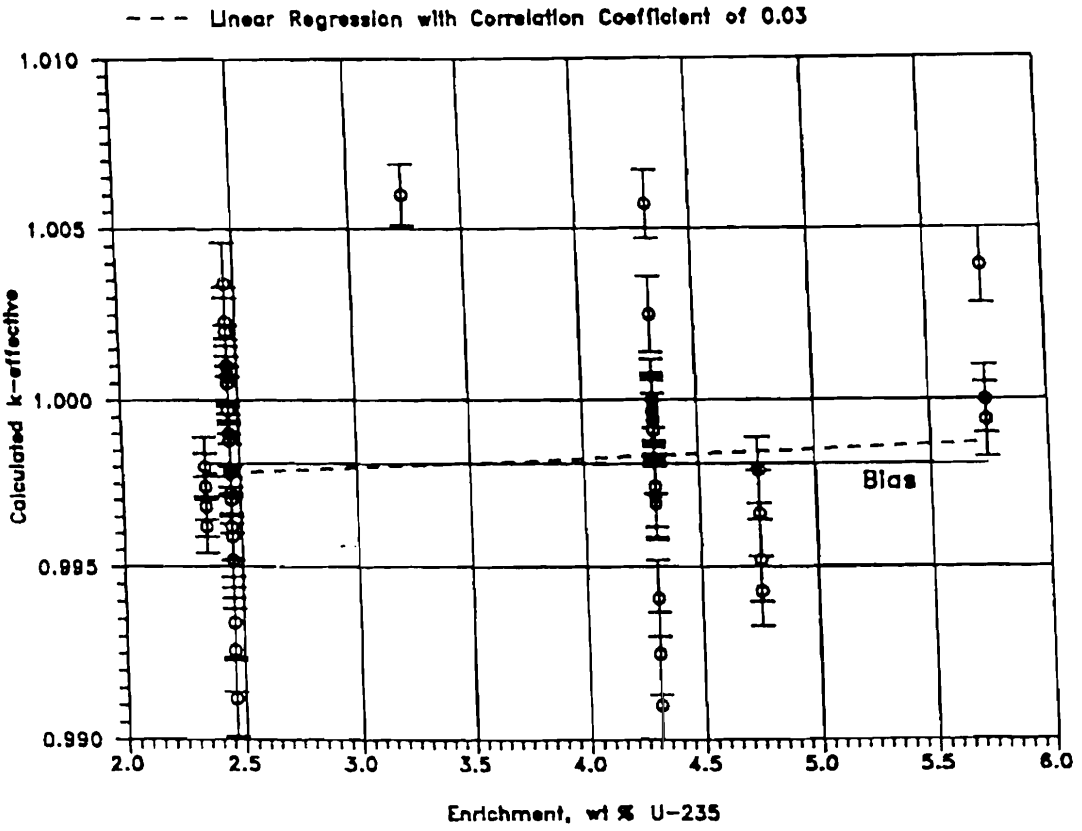

FIGURE A.3 MCNP CALCULATED k-eff VALUES
AT VARIOUS U-235 ENRICHMENTS

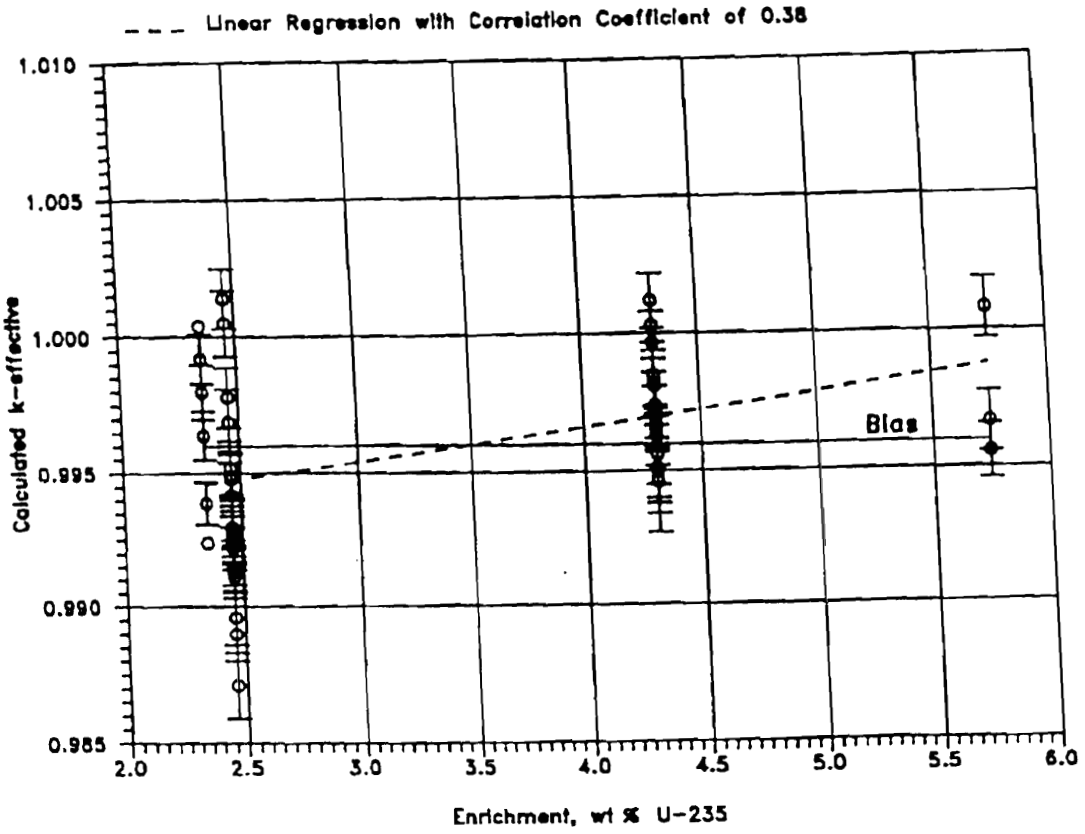

FIGURE A.4 KENO CALCULATED k-eff VALUES
AT VARIOUS U-235 ENRICHMENTS

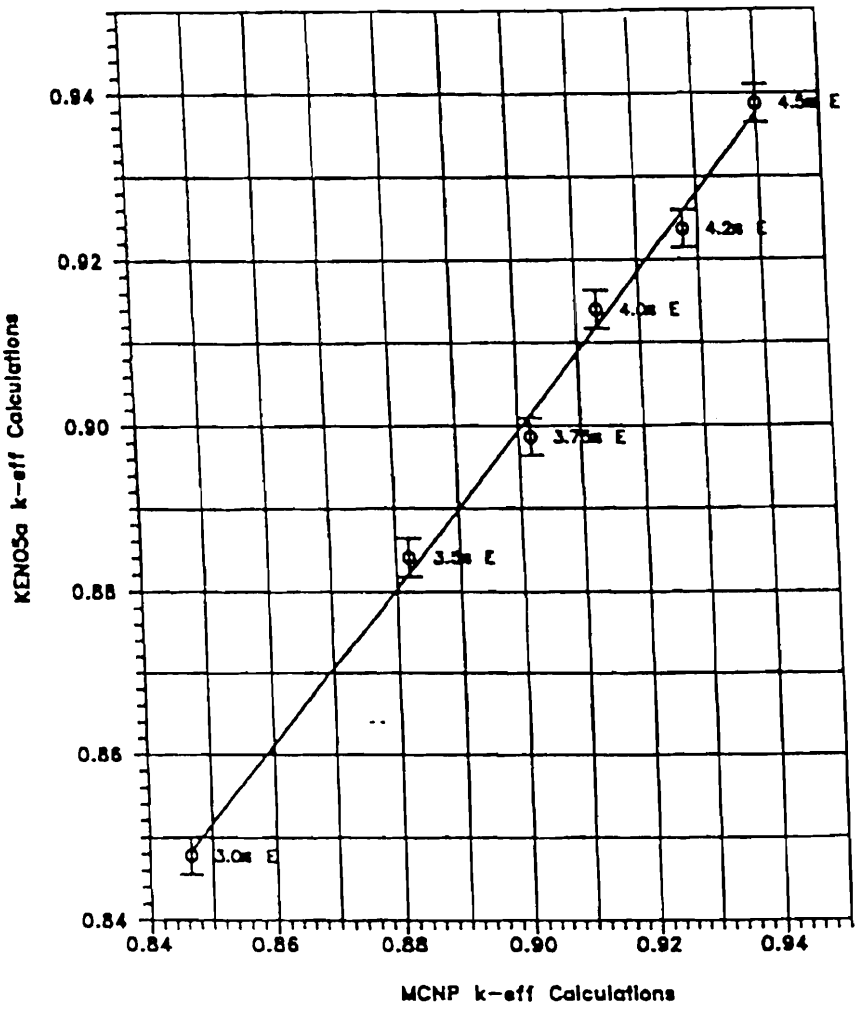

FIGURE A.5 COMPARISON OF MCNP AND KENO5A CALCULATIONS FOR VARIOUS FUEL ENRICHMENTS

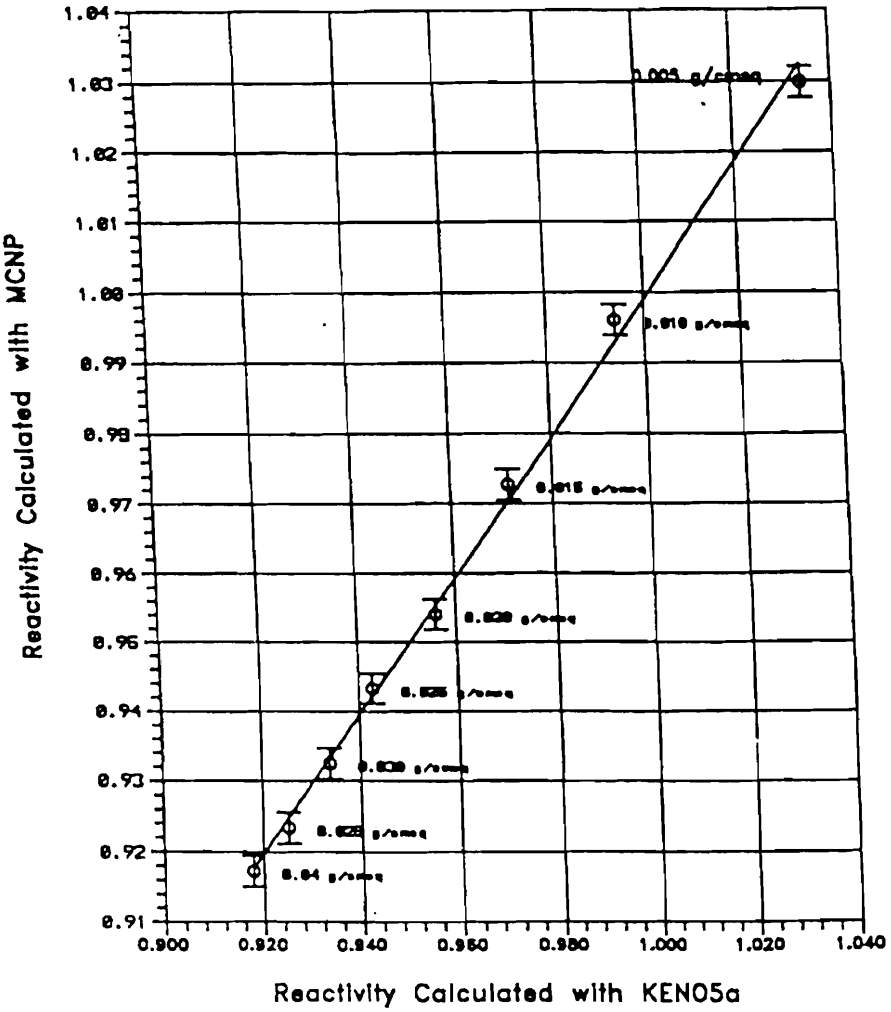

FIGURE A.6 COMPARISON OF MCNP AND KENO5a CALCULATIONS FOR VARIOUS BORON-10 AREAL DENSITIES

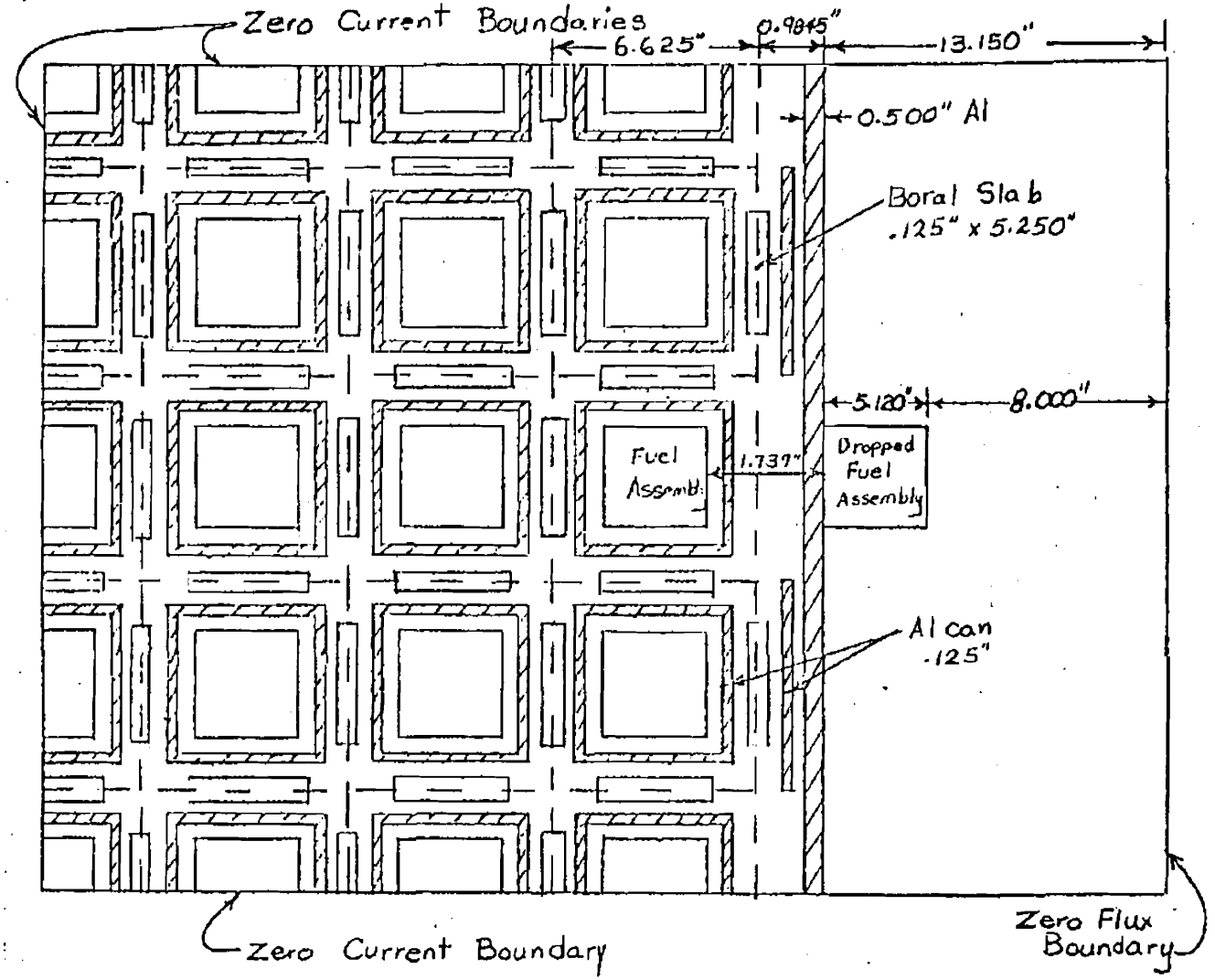

PIGURE 9 DAEC BWR Spent Fuel Storage, Dropped Fuel Assembly Accident

NAI 77-86
Revision 0
November 16, 1977